

CRANFIELD UNIVERSITY



MSc AEROSPACE COMPUTATIONAL ENGINEERING

Group Design Project: Modelling of Rapid Decompression of Civil Airliners

Authors:

Charles AUBERT
Marin LALLEMAND
Thibault LE SEGUILLON
Sévan RÉTIF
Giorgio SOGGIU
Rafi SUNTOURIAN

Supervisor:
Dr. Panagiotis TSOUTSANIS

April 17, 2021

Abstract

The aim of this group project is to study the effects and consequences of a depressurization on the cabin of a commercial airliner by performing CFD simulations. The pressure on the walls of the cabin of the airplane is studied in the case where a door or a window break during the flight. In this work, we mainly assume the flow to be unsteady and compressible, and the air being an ideal gas. The influence of numerous parameters being the altitude, mach number or opening shape is taken into account for the time evolution of the pressure. Several physical models are tested such as inviscid model in most of the simulations, but some RANS models has been investigated as well. The final goal of the investigation is to see if the pressure inside the cabin will stay reasonable for the materials of the walls which is part of the certification requirements for the airplanes. Models in two dimensions (A350 sized cabin with different opening), but also a simple model in three dimensions (only with the cabin and door of an A350) are used for the simulations. A validation of the profile of our results is done thanks to the existing literature. Investigations showed the existence of local pressure peaks despite a smooth global depressurisation on the cabin walls. Moreover, it has also been shown that the nature of the opening strongly impacts the pressure behaviour. External flying parameters such as the altitude or the Mach number also have a not negligible influence. We also highlighted that a low pressure zone forms downstream the opening. Furthermore, some of the results are more or less affected by the choice of the mesh which can create oscillations. Finally, the behavior of a 3D geometry model was confronted with a 2d model, the comparison between 2D and 3D models revealed that the 3D model shows a slower decompression than the 2D model and a different behavior for pressure peaks. Given the lack of references, it was not possible to determine if the more complex 3D model brings much realism to the results.

Acknowledgments

Thank you to James Plummer for his thesis project which is an excellent source of inspiration and has been a solid foundation for our work. Thank you to our supervisors Dr.Panagiotis Tsoutsanis and Dr.László Könözsy for their support and scientific guidance. A thank you also to Taryn Wylie for her precious encouragements and advice in term of organization in this challenging times.

These factors have been the keys to the successful completion of the project.

Contents

1	Introduction	6
2	Methods/Procedures	7
2.1	Meshing	7
2.1.1	Mesh geometry and boundary conditions	7
2.1.2	Physical model and set up Fluent	9
3	Results Giorgio	11
3.1	literature review (validation oriented)	11
3.2	Validation	13
3.2.1	3D mesh	13
3.2.2	2D mesh	13
3.3	Simulations	15
3.3.1	Global versus Local measurements	15
3.3.2	Refinement	18
3.3.3	peak	22
3.3.4	Window, Influence of the opening size	23
3.4	section's outcomes	23
4	Results Charles	24
4.1	Mesh choice and convergence study	24
4.1.1	Mesh refinement and results	24
4.1.2	Relative differences	26
4.1.3	Grid Convergence Index	27
4.2	Influence of the altitude on the decompression	28
4.2.1	Investigation of Average and Maximum Vertex pressure	32
4.2.2	Investigation of the pressure on door frame and exterior effects	33
5	Results Thibault	36
6	Results Rafi	40
7	Results Sévan	43
7.1	Parameters and their impacts	43
7.2	Structural approach with the pressure load	45
8	Results Marin	51
8.1	Study on the maximum pressure	53
8.2	3D mesh	55
9	Future work	61
10	Conclusion	62
11	References	64

List of Figures

1	2D Geometry	8
2	Extract from reference [4]	11
3	Extract from reference [4]	12
4	Extract from reference [3]	12
5	3D mesh Validation	13
6	Pressure history inside the cabin, door (length: 126cm)	14
7	Cabin, measurement points, locations	15
8	Pressure history and peaks prominence 200 at specific locations (point 1, 2 and 3)	16
9	Pressure history and peaks prominence 200 at specific locations (point 4 and 5)	17
10	Pressure history and peaks prominence 200 at specific locations (point 6 and 7)	17
11	Window(length:22.8cm), dt:0.01, 300 iterations, cabin pressure history, coarse/medium and fine mesh	19
12	Window(length:22.8cm), dt:0.01, 300 iterations, Wall 4 focus, pressure history,tendencies, coarse/medium and fine mesh	19
13	Window(length:22.8cm), Wall 4 focus, oscillations history, coarse/medium and fine mesh	20
14	Window(length:22.8cm),dt:0.01, 150 iterations, pressure differential between point measurements	20
15	Window(length:22.8cm), pressure tendency, coefficient of variation, fine mesh's gain	21
16	Window(length:22.8cm), coarse/medium fine mesh, pressure peak focus	22
17	Window(length:22.8cm), pressure peak, coefficient of variation, fine mesh's gain	22
18	Window size 1 (length: 22.8 cm),Window size 2 (length: 26.8 cm),Window size 3 (length: 30.8 cm), dt:0.01,iterations	23
19	Average pressure results for different mesh refinements	25
20	Evolution of the relative error between coarse, medium and fine meshes	26
21	Vertex Average pressure results for different altitudes	30
22	Lost of Vertex Average pressure on Wall 5 with thresholds	31
23	Vertex Average and Maximum pressure on Wall 4,5,6	32
24	Vertex Average pressure on door frame Walls 2,8	33
25	Overall contour of Pressure	35
26	Vertex Average pressure on the exterior fuselage	36
27	Study on RANS models	38
28	Study on RANS models	39
29	2D Geometry and name of the walls of the two cargo compartment	40
30	Pressure curves on the front and back cabin walls	41
31	Pressure curve on the side cabin wall (Wall 2)	41
32	Pressure curves on the Walls next to the opening zone	42
33	Different pressure zones next to the cargo opening compartment	43
34	pressure evolution for all the cases	44

35	Minimum value of static pressure on Wall5-a	45
36	First estimation of the maximal pressure load	46
37	Estimated maximum pressure load with a window (0.3m)	46
38	Estimated maximum pressure load with a door (1.27m)	47
39	Estimated maximum pressure load with a cargo door (3m)	47
40	First estimation of maximum pressure load for all the cases	48
41	Limitations of the first estimation of the maximum load	48
42	Impact of parameters on the time of the maximum load's apparition	49
43	Impact of parameters on the time of the maximum load's value	50
44	Impact of parameters on the time of the maximum load's position	50
45	Impact of the Mach number on the maximum load propagation	51
46	Impact of the opening size on the maximum load propagation	51
47	Study on RANS models	53
48	Study on the maximum pressure on the walls	54
49	View of the 3D mesh	55
50	Study on the 3D mesh	56
51	Study on the 3D mesh (2nd simulation)	58
52	Contours of pressure with the 3D model	59

List of Tables

1	Measurements points inside the Cabin and their coordinates	15
2	Number of peaks at specific locations, count performed during 6 seconds	18
3	Initial meshing definition	24
4	Relative error between the meshes	26
5	Convergence ratio	28
6	Outside air conditions	28
7	Cabin air conditions	29

1 Introduction

Throughout the aviation's history, reaching the highest altitudes was very usefull for many aspects. As the air becomes thinner with altitude, airplanes can flight faster with a reasonable fuel consumption. Moreover, the most of weather perturbations can be avoided in high altitudes, so the comfort and security are both improved. Unfortunately, the temperature tends to decrease with altitudes, and hypoxia effects appears above 10000fts, so the pilots can easily pass out (Flight 522 Helios Airways). While military airplanes use masks for supplying oxygen to the operators, a viable environment withing the fuselage is needed for commercial airplanes. The Boeing 307 Stratoliner, built in 1938, was the first pressurized airliner. Due to higher pressure inside the cabin, a sudden depressurisation is a probable risk, and several accident have already occurred,(example: Turkish Airlines Flight 981). The depressurisation mostly occurs at a cruising altitude and speed, about 35000fts and 250m/s for an Airbus A350. This study aims to investigate the impact of a depressurisation by simulating two-dimensional simplified model. The CFD simulations have used a two-dimensional approach is a air-pressurized box in contact with a far-field of constant-Mach air-flow. The Mach number chosen for the simulations is high ($Ma=0.82$) so the compressible effects of the fluid can not be neglected, and the simulations have to be performed with a density based method. The inviscid flow approximation has been chosen for simulating the compressible flow involved in this study. For an inviscid assumption the momentum equation can be written as following (1):

$$\frac{\partial \rho u}{\partial t} + \rho(u \cdot \nabla)u = body forces - \nabla p \quad (1)$$

ρ being the density, u the velocity field of the flow and p the pressure field, the momentum is able to link the variations of the velocity and the density with pressure variation only. For the two-dimensional problem, the gravity force is neglected as the considerate surface is supposed to be horizontal. As any other body force is considerate, the right hand side will only contained ∇p . It means that the shear forces caused by the viscosity are neglected. Several opening are involved on a commercial such as the doors, the windows or the cargo door, so the depressurisation is expected to be different in function of the opening concerned. This study is centred of the pressure evolution during a depressurisation, the parameters such as the altitude, the Mach number, the size of the opening and its position are investigated in order to study their impact on the pressure evolution. Finally, the impact of the pressure perturbation on the structure has been discussed, such as oscillations due to flow close to the opening, or pressure load calculated on the walls.

2 Methods/Procedures

2.1 Meshing

2.1.1 Mesh geometry and boundary conditions

The Figure 1 hereafter represents the 2D geometry defined for our study. In order to run various simulations, 2 types of meshes are defined with different software. The first mesh is a structured mesh created with ICEM (Figure 1a) while the second mesh is unstructured and created with Workbench (Figure 1b). These meshes are the base meshes used in this report. The choices are deeply explained in the Physical model and set up part of this report.

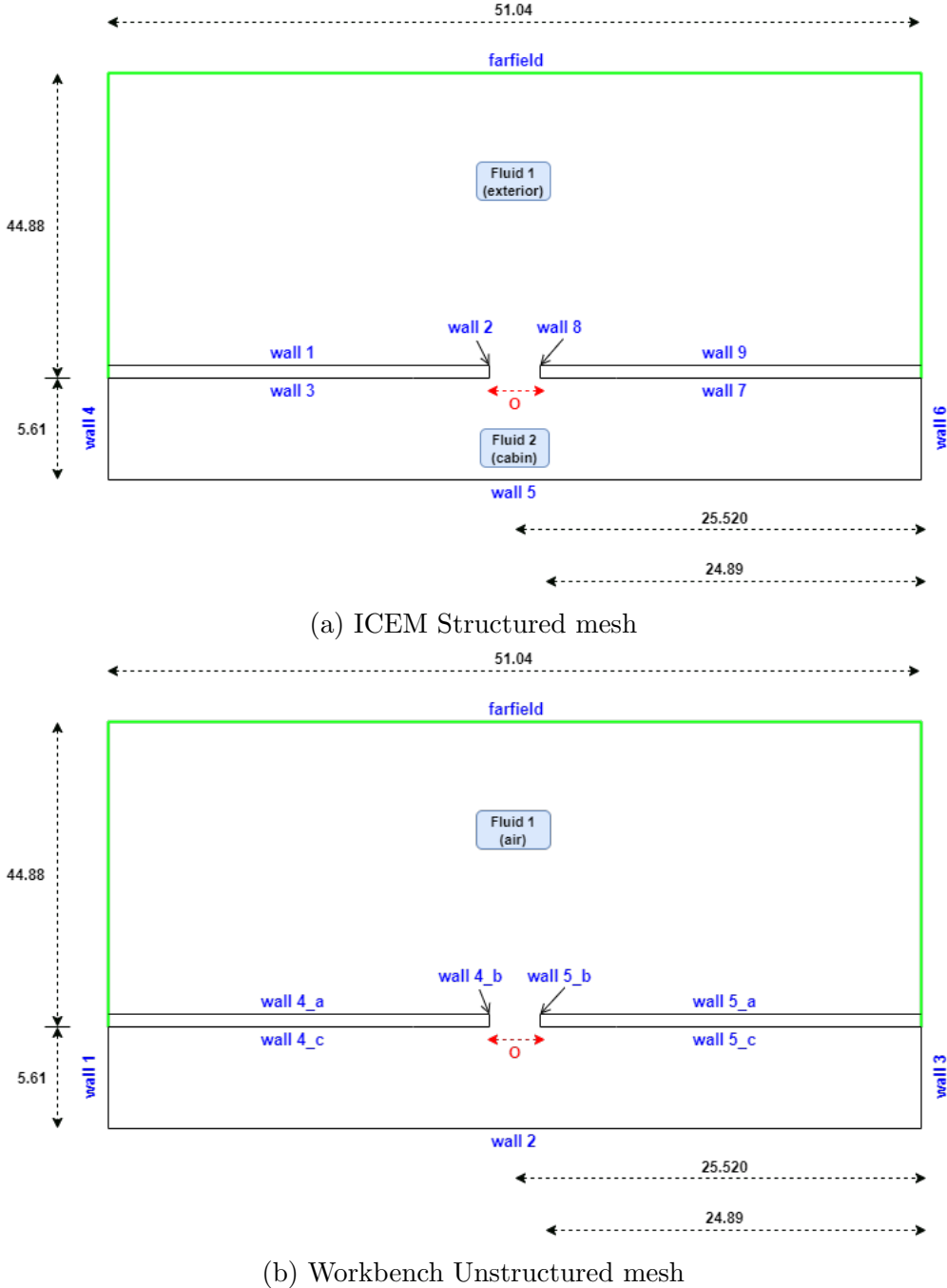


Figure 1: 2D Geometry

This 2D cabin model is designed to have the same dimensions as an Airbus A350-900 cabin with data obtained from the official documentation [1].

The geometry is separated between a cabin part and an exterior part. 2 different fluids are defined in the mesh, the Fluid 1 is defined for the exterior and get the properties of the air outside the plane at cruise level in ISA conditions. The Fluid 2 is defined for the cabin and has initially the properties of pressurized air for passengers and crew. Trivially, the air of the cabin has a much higher pressure and temperature, which is equivalent to a lower pressure altitude in ISA conditions, than the outside air.

Between the cabin domain and the outside, an opening of parameter O is defined. In our different studies, the parameters O will be changed in order to simulate a window, a door or a cargo door.

2.1.2 Physical model and set up Fluent

In this section, we are going to explain the physical model we use for our numerical simulations, and the specific setting under Fluent to set up correctly this model. The first point is that we are working with an unsteady flow, which means that our flow is a function of time. That will allow us to observe the variation of the average pressure inside the cabin through the time. Then we are working with a compressible flow, which means that changes in the density are big enough to be taken into account. These two points are the baseline model we are working on.

The physical model is an essential choice to deal with Navier-Stokes equations and run correctly the simulations. According to our tutor and the thesis dealing with our problem, an inviscid model seems to be the one to work with. The point is to neglect the viscosity and a possible turbulence. With that model, we indicate to Fluent that we want to solve the energy equation as well (energy equation ON), and we choose to work with an ideal-gas for the air.

For the boundary conditions, we work with the following settings for the farfield, the rest of the boundaries being walls :

- a Mach number of 0.82
- a gauge pressure of 25 000 Pa (Approximately the Pressure of the atmosphere at the altitude we chose to work with)
- a temperature of 225K (Approximately the temperature of the altitude we chose to work with)
- Same direction for the flow and the airplane (direction x in Fluent) !
- An operating pressure of 0 Pa to be coherent with the real pressure

Concerning the methods for the numerical part of the simulation, we tried different settings and chose the following ones : an explicit formulation, the ROE-FDS solver, the Least Square Cells Based method with a second order scheme for the flow, and finally a second order implicit scheme for the transient formulation.

What we are interested in is the evolution in time of the average pressure on the walls. To calculate that with Fluent, we had to use " Report Definitions ", create a Surface Report and choose to calculate the Vertex Average for the walls inside the cabin. The vertex average of a specified field variable on a surface is computed by dividing the summation of the vertex values of the selected variable by the total number of vertices. We create a file containing this average value at each flow time for each wall, in order to post-process the data.

The initialization is a bit specific for our study. Indeed, we have to set up the pressure outside but also inside the cabin to have the good conditions of simulation. We use as always a standard initialization, compute from the Boundary conditions Farfield. Then

we use the option Patch to set up exactly our values for the pressure, the velocity and the temperature outside and inside the cabin ! Inside the cabin, we consider that the pressure is equal to 85000 Pa and the temperature equal to 293K. The last point is the parameters for the run calculation. We made the choice to work with a time step size of 0.001, a number of time step of 3000 and max iterations/time step of 80.

3 Results Giorgio

3.1 literature review (validation oriented)

Alfonso Pagani and Erasmo Carrera have performed a cabin decompression analysis [4] on two different aircrafts and different breach size. The breach apparition is considered as instantaneous. The cabin is modeled as a single-chamber and a siloed chamber. The problem is treated with a diabatic and reversible isentropic process. The simulations' perimeters respect assumptions of constant fuselage volume during decompression and external atmosphere infinity. Air is considered as an ideal gas. Moreover external pressure fluctuations are neglected. The study focuses on pressure density and temperature evolution through time.

Table 1 Decompression times of the single chamber

	Supercritical phase duration $\frac{t_{sup}}{V/A} \times 10^3 \left(\frac{s}{m} \right)$	Subcritical phase duration $\frac{t_{sub}}{V/A} \times 10^3 \left(\frac{s}{m} \right)$	Total decompression time $\frac{t_{tot}}{V/A} \times 10^3 \left(\frac{s}{m} \right)$
Present model	3.23	3.82	7.05
Daidzic and Simones (2010)	3.23	3.95	7.18
Haber and Clamann (1953)	4.43	4.09	8.52

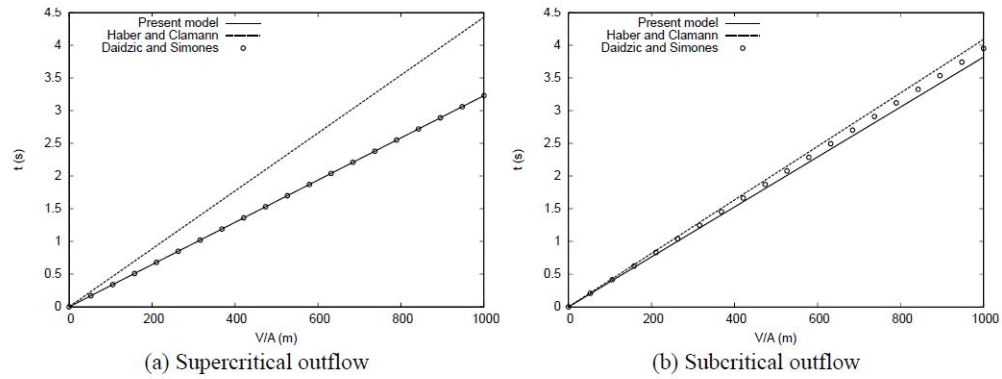


Fig. 4 Supercritical and subcritical phases durations of the single chamber for various V/A ratios

Figure 2: Extract from reference [4]

The subcritical phase duration of the decompression is presented as a function depending on the V/A ratio (with V the cabin volume and A the breach area). Physical parameters used: single chamber volume = 4m³, initial pressure=117.013kPa,initial temperature=23C. ambient pressure 26.4289, ambient external temperature =-50C.

Subcritical phase duration increases as the ratio increases. Obtained results are in adequacy with those obtained from studies using a polytropic and isentropic model. Models' impact is more noticeable on Supercritical flow. Polytropic is recommended for longer decompression.

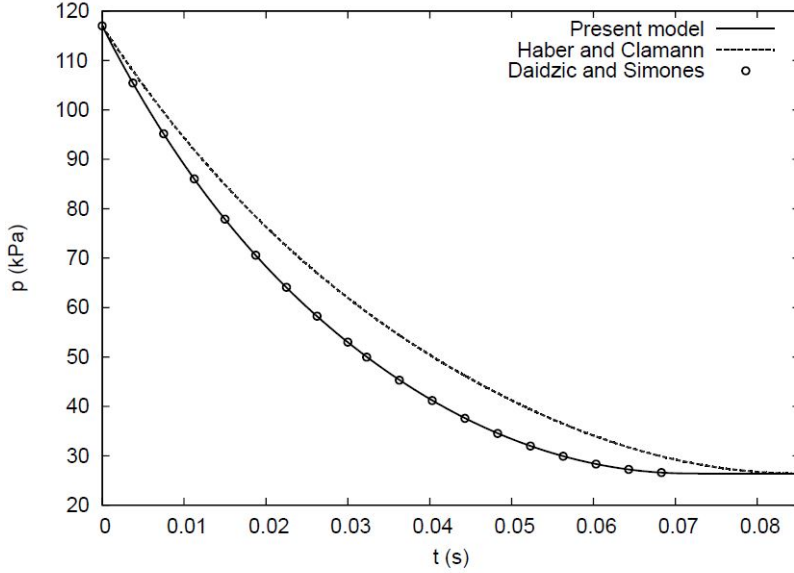
Fig. 5 Pressure history within the single chamber for $V/A=10$ m

Figure 3: Extract from reference [4]

The pressure evolution for $V/A=10$ m is depicted in the fig 5. The evolution is considered as "smooth" without oscillations. The regular (no oscillations) tendency of the pressure curve will be considered as a positive criteria for both Validation and quality purposes.

Nihad E.Daizdic and Matthew P.Simones have developed a zero-dimensional model of cockpit for an analysis [3] based on an isentropic and isothermal model. Different cabin geometries, pressure altitudes among others parameters' impact are studied. The attention is focused on total decompression time and for convenience pressure half-time. Cockpit integrity considering (decompression) and passengers security are at the heart of the study.

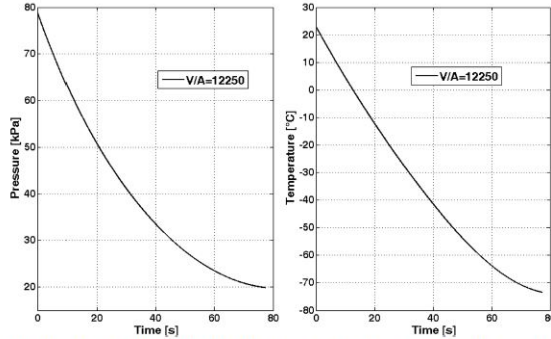
Fig. 9 Boeing 767-300ER cabin pressure and temperature history for closed cockpit door, cabin rupture of 0.1 m^2 .

Figure 4: Extract from reference [3]

The cabin endures a decompression due to a fuselage rupture of $0.1n^2$. In 80 seconds, the pressure has dropped from about 79 000 Pa down to 20 000.The evolution history depicts a non oscillatory behavior. Data obtained are digitalised and used in the Validation section to test the 3D mesh.

3.2 Validation

3.2.1 3D mesh

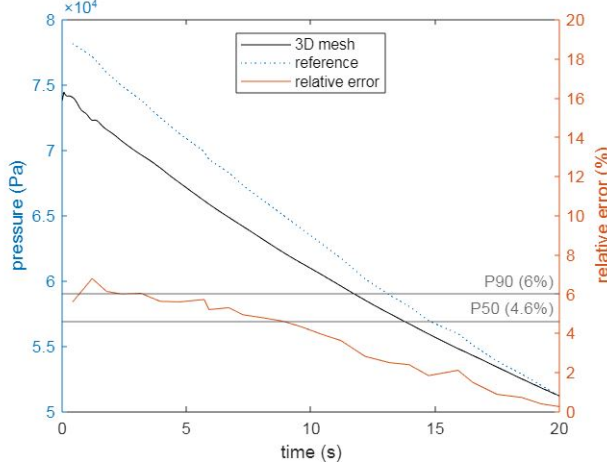


Figure 5: 3D mesh Validation

The above figure shows the pressure evolution for both reference and current simulation (using 3D mesh). The 3D mesh performed via ICEM is described in Marin's section. The simulations is performed with parameters similar to those used in the work of Nihad E.Daizdic and Matthew P.Simones. Geometry from reference and the current mesh differ in term of volume and opening area. This difference is counteracted by the equation provided in [4] which bring a ration (V/A).

Qualitatively, can be noticed that our model suffers from a lack of accuracy in term of pressure and pressure drop during the first seconds. This negative aspect is progressively corrected as time goes by. Globally a common behavior in term of tendency is noticeable. First 10 seconds highlight divergences as materialised by the curve of relative error which reaches its maximum around 1 sec. 95% of errors are smaller or equal to 6%. Moreover Percentile 50 reveals that 50% of error are smaller or equal to 4.5% which is a positive indicator. Additionally no major discrepancies are visible in term of oscillations. Both curves are "smooth".

Minor discrepancies could be explained by remaining uncertainties such as mesh parameters differences which have not been taken into account while performing the 'like-for-like' simulations. As relatives errors are small despite uncertainties and tendency globally similar to the reference, **the 3D mesh is considered validated**. The 3D mesh is reduced into a 2D geometry which is used in the current study in parallel of the 2D mesh created using Workbench.

3.2.2 2D mesh

A simulation is performed using the 2D mesh. Pressure history inside the cabin is represented on the cabin's five walls and at a point in the middle of the cabin.

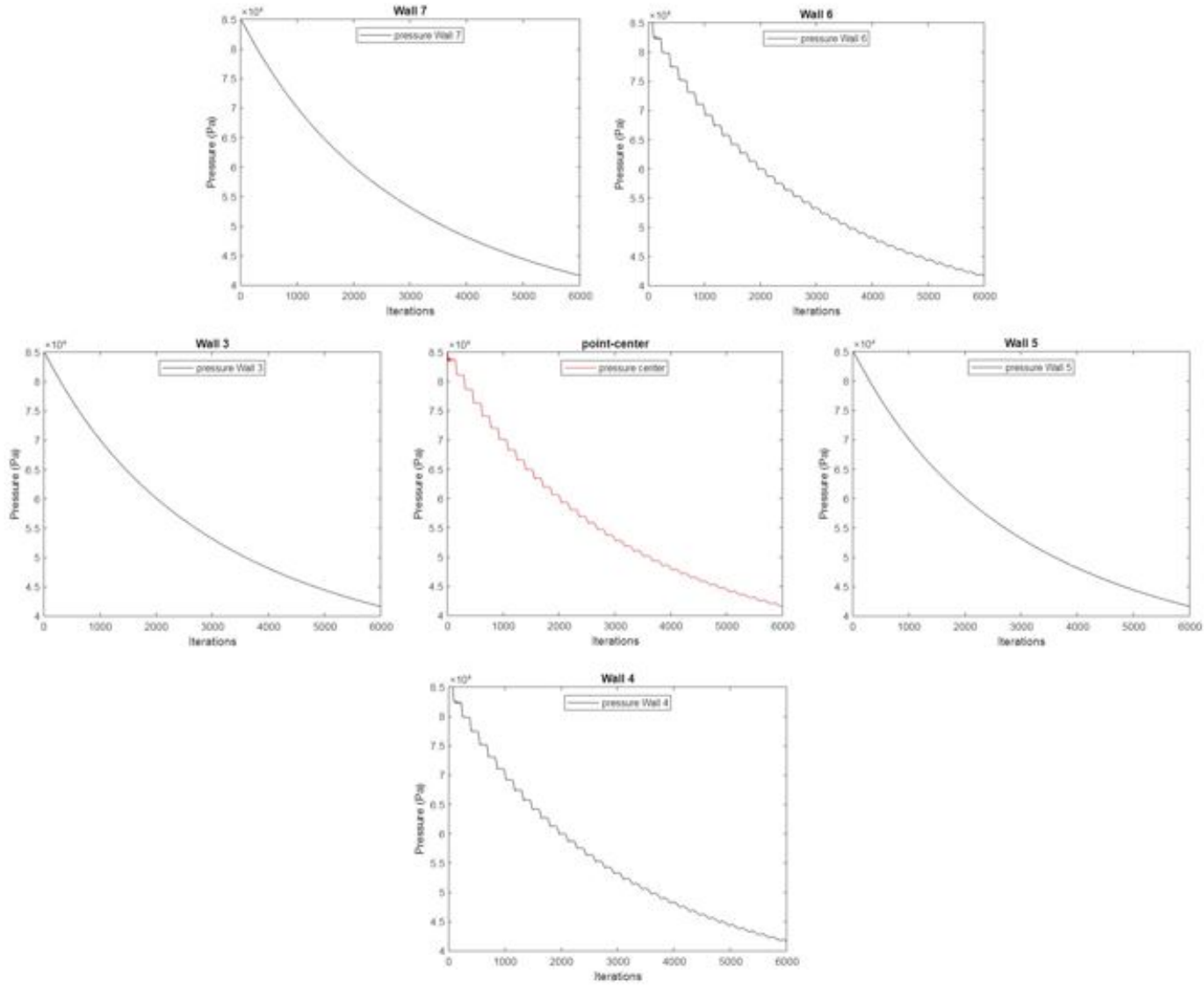


Figure 6: Pressure history inside the cabin, door (length: 126cm)

The first striking aspect is the similar behavior of the pressure in the different locations presented. In term of tendency, curves do not differ from each other and correspond visually to references [4] and [3].

A quantitative approach is not possible as references are in 3D, nevertheless, qualitatively, results are in accordance with expectations from references. **The 2D mesh is then considered as a positive foundation for upcoming studies.**

Nota: The cabin is symmetric and this element is put forward comparing walls 3 and 5. Oscillations are noticeable at walls 6 and 4. At a first stage the obtained results do not explain the apparition of these oscillations at these walls. Creating a measurement point at the center of the cabin does not bring further information. However if we were able to reduce the oscillatory behavior, results obtained at this point would be a good // average/summary of walls' results.

3.3 Simulations

Before performing the full range of simulations, the question of how to measure and take the pressure information is raised. A brief comparative study is performed on the door to identify whether wall or local measurements give the most conclusive results. This brief analysis is performed on a 2D mesh with a door as opening (Length:22.86 cm). **We question the pertinence of local measurements via point versus global measurements via Wall study.**

Nota: the complete study of the door is performed and described in Thibault's section.

3.3.1 Global versus Local measurements

Measures are then taken at specific locations. The following table gives their coordinates. Three measurement axes are visible in (Figure 7): 2 verticals and 1 horizontal. Verticals are respectively parallel and close to wall 7 and through the opening.

point number	Coordinates	
	x	y
1	0,1	5,11
2	0,1	4,61
3	0,1	3,61
4	0,1	2,805
5	0,1	2
6	0,1	1
7	0,1	0,5
8	25,52	2,805
9	25,52	5,56
10	25,52	5,61
11	50,94	2,805

Table 1: Measurements points inside the Cabin and their coordinates

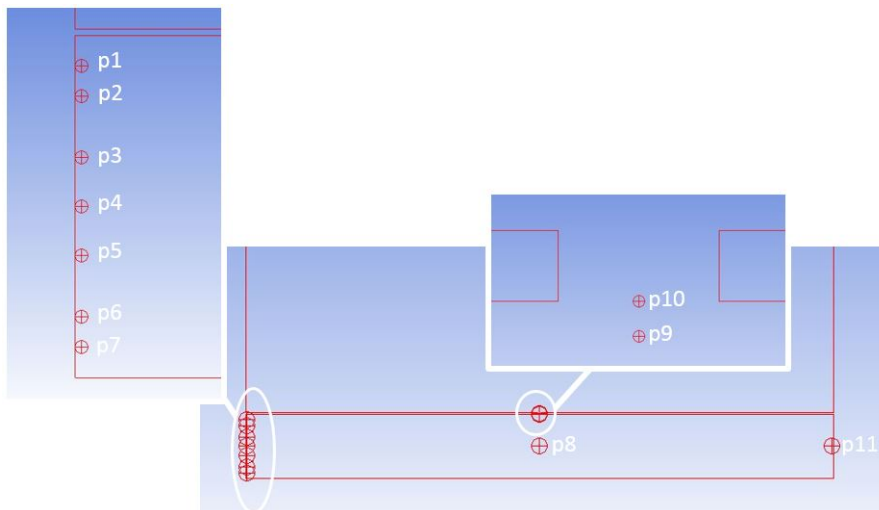


Figure 7: Cabin, measurement points, locations

By focusing on wall 3 (left side of the cabin) and points localised close to it (Figure 7:p1 to p7), can be noticed a similar behavior in term of tendency. Nevertheless, pressure history obtained through points measurements are not as smooth (more oscillations) as those obtained via wall measurements (Figures 8, 9 and 10). Oscillations are identified highlighting pressure peaks having a prominence superior or equal to 200. **The question is: are the oscillations a physical behavior or computational errors?**

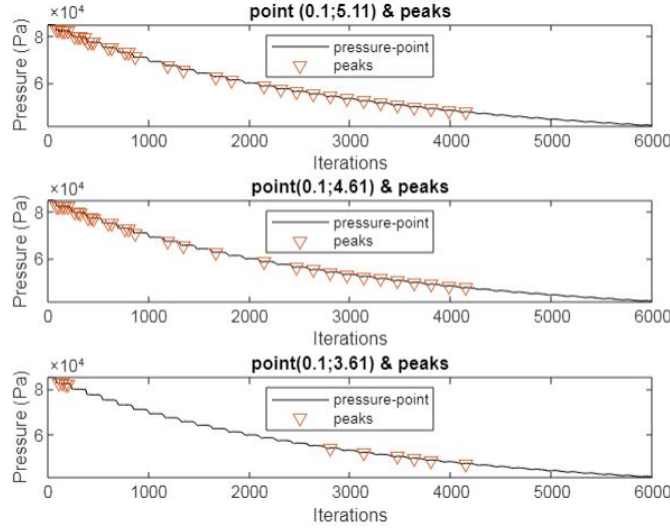


Figure 8: Pressure history and peaks prominence 200 at specific locations (point 1, 2 and 3)

The above picture shows the pressure history through time at point 1, 2 and 3. Pressure peaks of prominence 200 are highlighted. At point 1, peaks are noticeable from the first to 4200 iterations, Peaks distribution is almost continuous with higher density at the beginning of the simulation and lower density around 1500 iterations. After 4200 iterations, no peaks are visible.

At point 2, a similar behavior is noticeable. The lower density zone around 1500 iterations is also existing and looks slightly less provided in term of peak than for point 1.

At point 3, the lower density zone disappears creating two distinct zone of higher peak density. Peaks are visible at the start of the simulation (at the first iterations). Few peaks are visible around 300 iterations. Peaks density in this specific area is weaker than for point 1 and 2 at same iterations.

Peaks' distributions do not differ visually significantly between point 1 and 2. Point 3's distribution stands aside.

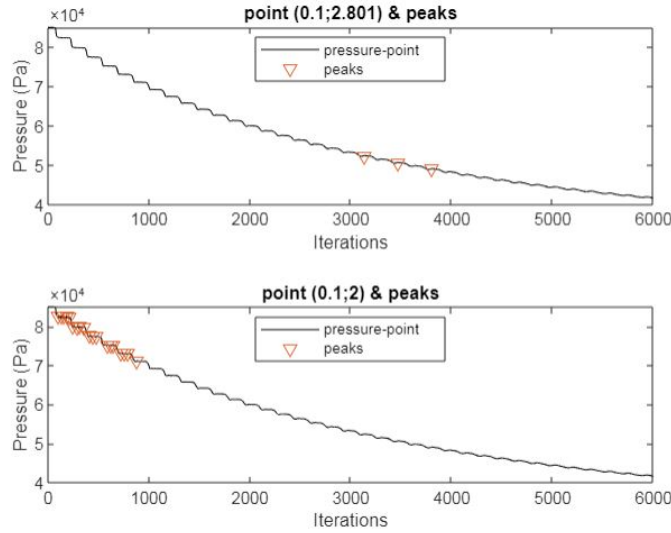


Figure 9: Pressure history and peaks prominence 200 at specific locations (point 4 and 5)

Point 4 (Figure 9), at the center, seems less impacted by the oscillatory phenomena. Indeed 3 peaks are visible between 3000 and 4000 iterations and none at the beginning of the simulation. Point 5's graph (Figure 9) brings the reappearance of peaks at the beginning of the simulation from the first to 1000 iterations.

Point 6 (Figure ??); peaks are localised in the smaller area (first to 500 iterations).

Point 7 (Figure ??); peaks are localised from the beginning of the simulation to iteration 1000. The pressure history peaks distribution at point 7 acts similarly as for point 5.

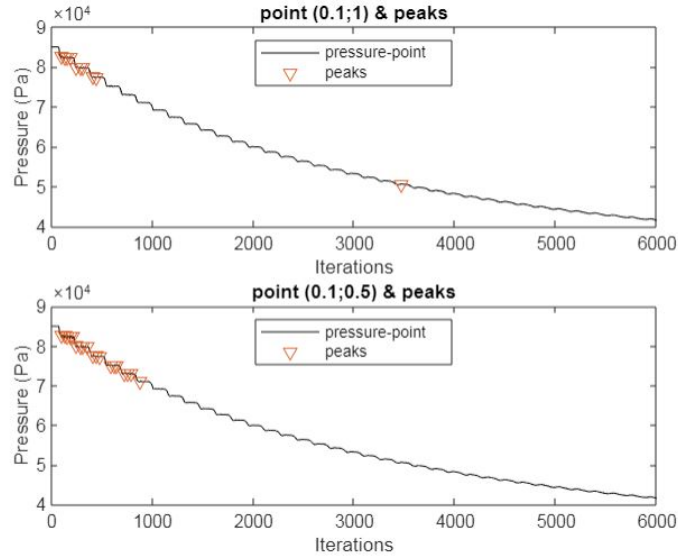


Figure 10: Pressure history and peaks prominence 200 at specific locations (point 6 and 7)

	peaks (prominence 200)count
Wall 3	9
point (0,1;5,11)	34
point (.01;4,61)	31
point (0,1;3,61)	10
point (0,1;2,805)	3
point (0,1;2)	19
point (0,1;1)	10
point (0,1;0,5)	1

Table 2: Number of peaks at specific locations, count performed during 6 seconds

In the above figure, the number of peaks having a prominence superior or equals to 200 is counted for points and wall3. No relationship is visible between peak distribution and the geometry of the cabin (Figure ??). The origin of peak density evolution over time is not explained in our study. This, in appearance, '**erratic' distribution**' and the non conformity in term of smoothness compared to reference, gives a motivation to reduce the amount of peaks. **An attempt is performed using a refinement strategy to overcome oscillations so as to highlight eventual useful information 'behind' oscillatory perturbations.**

3.3.2 Refinement

Simulation is performed with a window (length:22.8cm). Simulations are performed using respectively a coarse, medium and fine structured mesh. The coarse mesh has 17749 Nodes and 17118 elements with squared cells with length 0.09 and 0.045 m. A medium mesh is created from the coarse mesh reducing the cell's by a factor of 1,5. The fine mesh is produced by applying the same factor to the medium mesh.

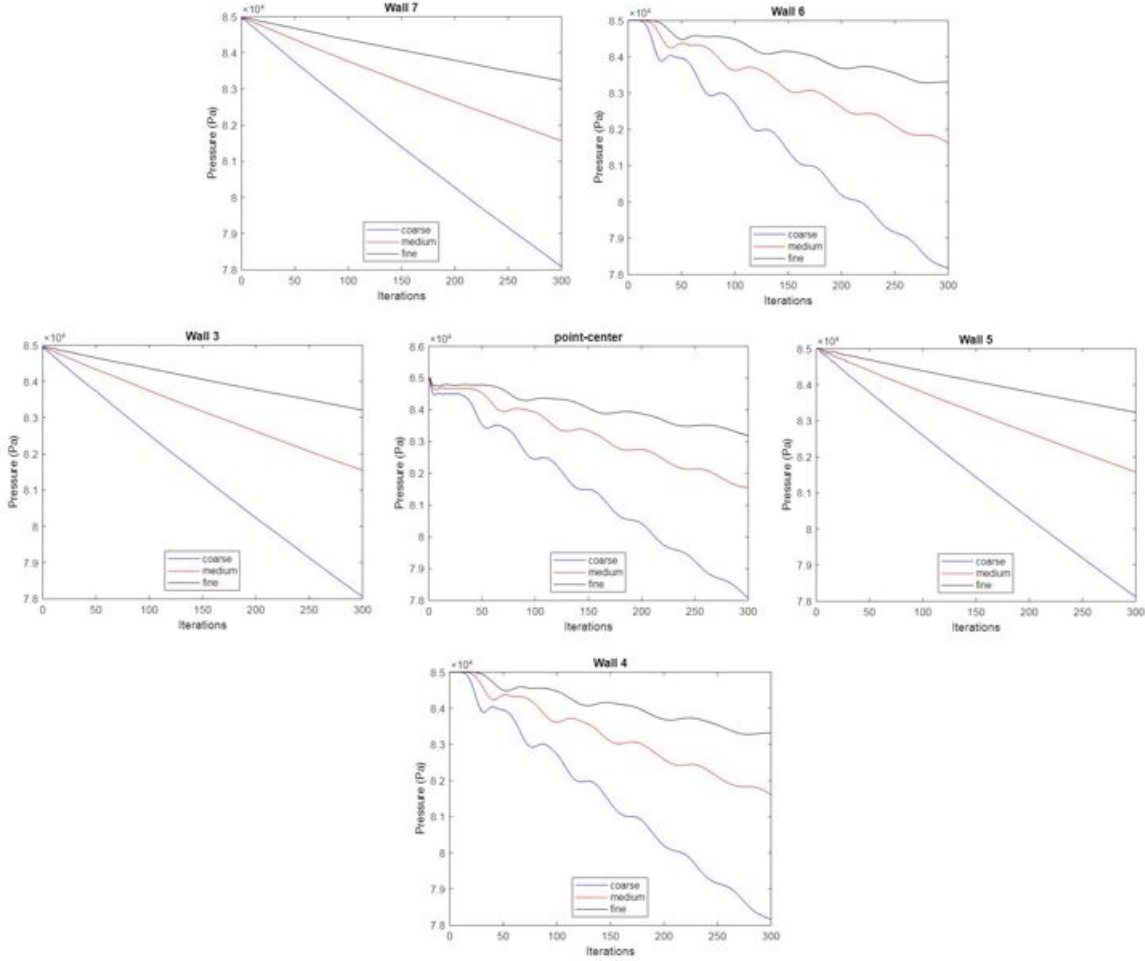


Figure 11: Window(length:22.8cm), dt:0.01, 300 iterations, cabin pressure history, coarse/medium and fine mesh

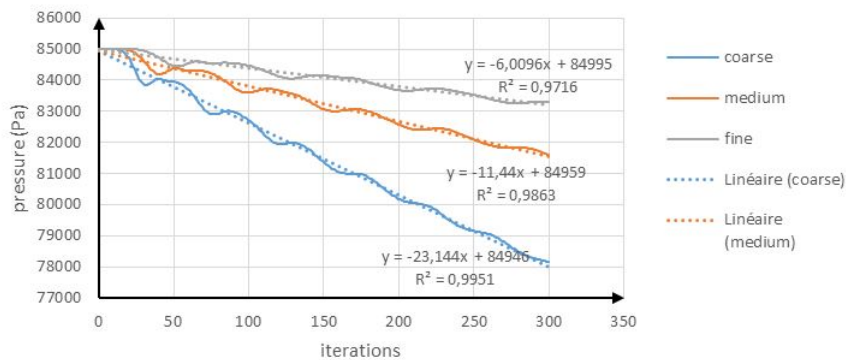


Figure 12: Window(length:22.8cm), dt:0.01, 300 iterations, Wall 4 focus, pressure history, tendencies, coarse/medium and fine mesh

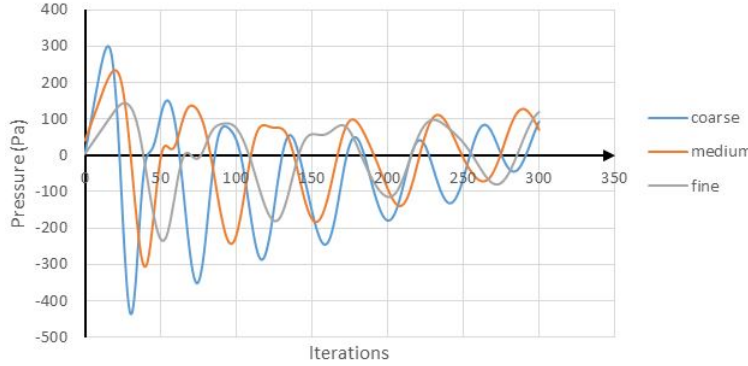


Figure 13: Window(length:22.8cm), Wall 4 focus, oscillations history, coarse/medium and fine mesh

The above figure isolates oscillations for wall 4 by subtracting to obtained data (figure11)their respective tendency. Oscillations are presented as relative to the tendencies of the the pressure history depicted in (figure13). The oscillations' magnitude are reduced as the mesh is refined. Once oscillations partly tempered via refinement an attempt is made to evaluate pressure differences between measurement points close to wall 3 and during the first 150 iterations.

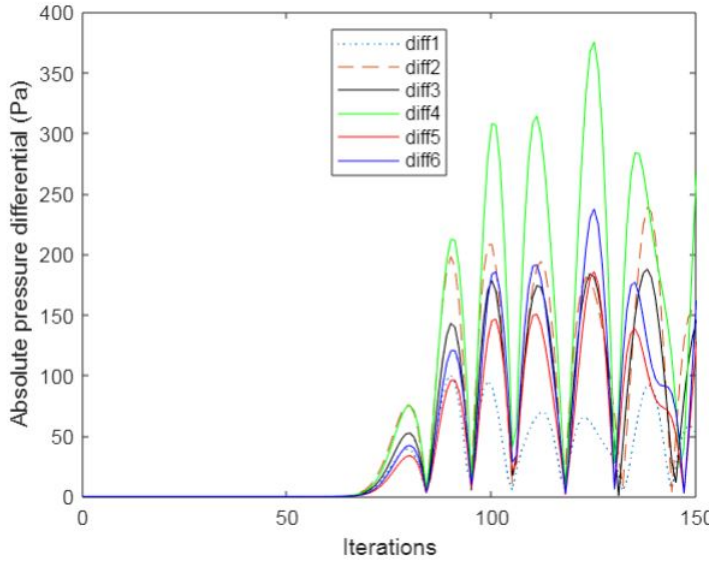


Figure 14: Window(length:22.8cm),dt:0.01, 150 iterations, pressure differential between point measurements

'diff1' corresponds to pressure differential between point 1 and 2, 'diff2' between point 2 and 3,... Evaluating differentials (figure14) reveals high pressure difference between points 4 and 5. This observation is not visible in Wall measurements using an averaging method. This finding shows that measuring pressure on walls ostracize information such as pressure differential which could be used with a structural study in order

to identify possible damages on the cockpit's door as in reference [4]. From that observation, **the idea of localised measurements makes sense** and will be used in Sévan's section. Nota: The study of wall measurements performances is continued in Charles' section where an investigation of the differences between Average and Maximum Vertex pressure measurement is conducted.

A second observation is visible: refinement generates impact on the pressure drop down rate. Working on linear curves' tendency bring to the fore differences in term of coefficient of variation (figure 12).

The pressure decreases on the simulation performed via the fine mesh is slower than via the medium and coarse mesh. The difference between the coarse and medium mesh looks more meaningful than the one between the the medium and fine mesh.

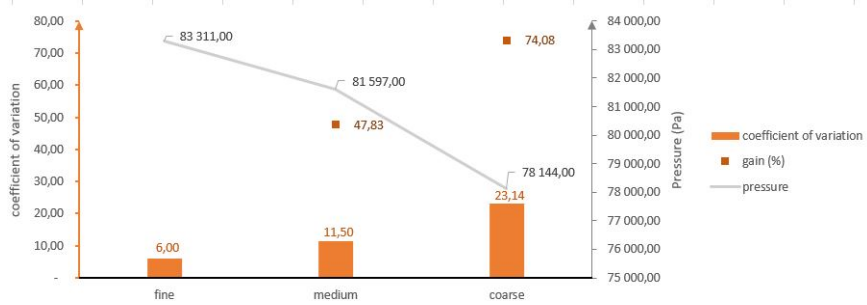


Figure 15: Window(length:22.8cm), pressure tendency, coefficient of variation, fine mesh's gain

Figure 15: Pressure obtained at time t equals 3s and coefficient of variations for simulations performed on coarse, medium and fine mesh are presented. Meshes are classified according to their results. The fine mesh which has the smallest coefficient of variation is considered as reference. The finest mesh's gains compared to the other meshes are given.

The linear tendency from the fine mesh has a coefficient of variation of 6 which is approximately 48% and 74% inferior to those from medium and coarse mesh. This indicator impact pressure results; after 300 iterations which corresponds to 3s, a pressure differential is noticeable. Where the pressure obtained on the fine mesh is roughly equals to 83311, it is equals to 81597 and 78144 on the medium and coarse mesh. These differences bring to the fore importance of refinement.

3.3.3 peak

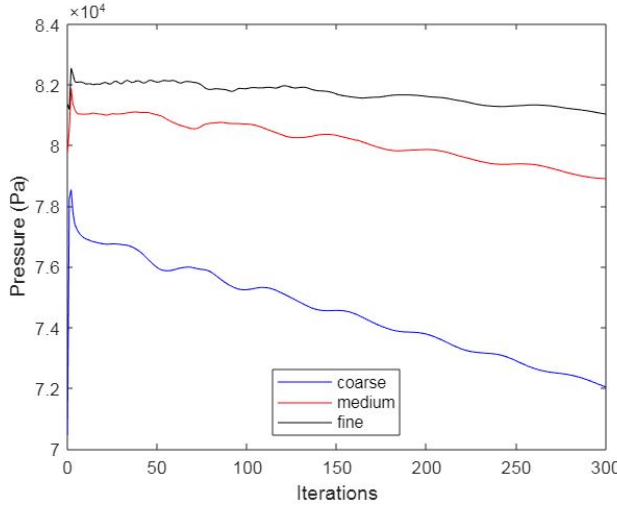


Figure 16: Window(length:22.8cm), coarse/medium fine mesh, pressure peak focus

On the coarse mesh (Figure 16), a pressure peak is observable at point 9. The maximum values obtained are smaller than cabin's initial pressure. This peak was not perceptible via Wall averages. It gives interest to 'point measurement'.

A similar phenomena is noticed in medium and fine meshes. Qualitatively, the peak pressure value increases and peak's prominence decreases as meshes get finer. Difference between coarse and medium is larger than the difference between coarse and fine.

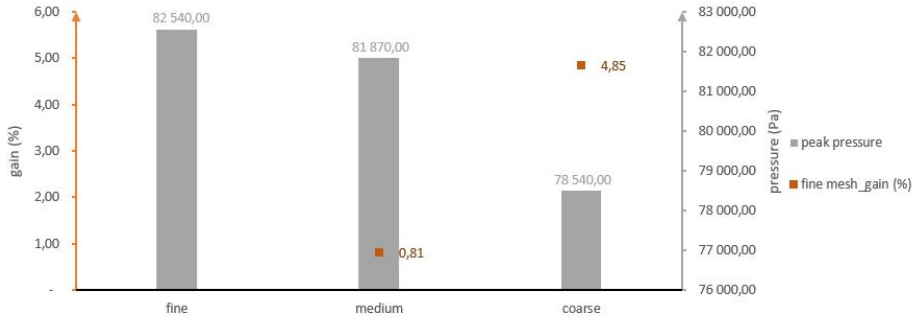


Figure 17: Window(length:22.8cm), pressure peak, coefficient of variation, fine mesh's gain

Figure 17: The peak pressure obtained on the fine mesh reaches 82540 Pa which is 0.81% higher than the peak on medium mesh (81870 Pa) and 4.85 % higher than the peak on coarse mesh (78540 Pa).

The refinement's impact on peak pressure is in accordance with previous results. **Refinement seems not to be ostracized in the current study.** A Grid Convergence Index is performed on Charles' section to evaluate accurately how to define meshes.

3.3.4 Window, Influence of the opening size

Simulations are performed with three different window length (22.8/26.8 /30.8 cm). We question the impact of length as performed in reference [3]. A similar global behavior behavior will be considered as another positive indicator for 2D mesh validation. A similar study will also performed by Thibault in his section.

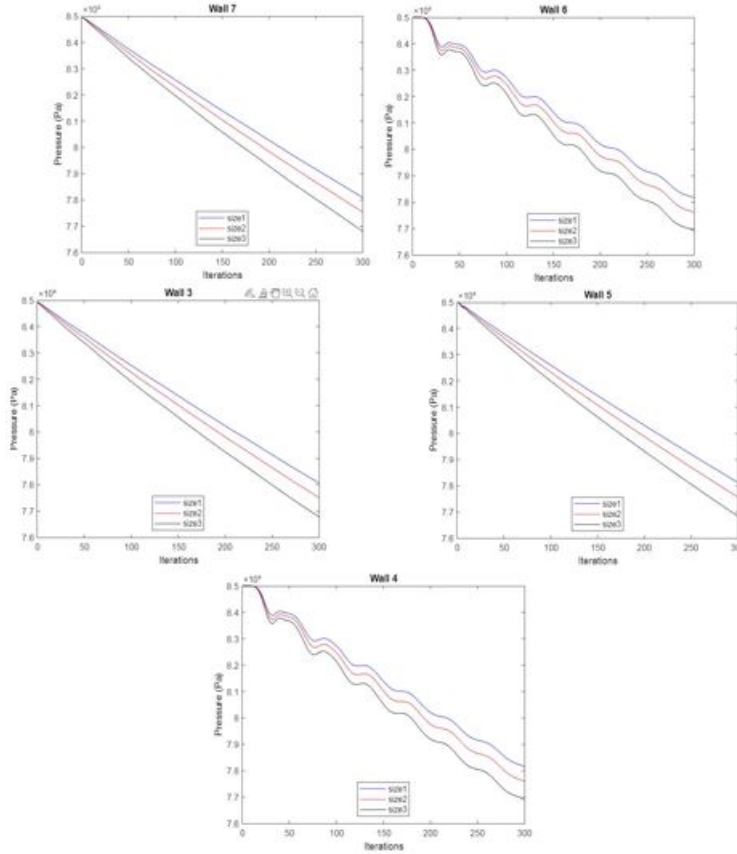


Figure 18: Window size 1 (length: 22.8 cm),Window size 2 (length: 26.8 cm),Window size 3 (length: 30.8 cm), dt:0.01,iterations

Figure 18 shows pressure history inside the cabin with three different windows. In this specific part we focus on the difference in term of pressure history due to different opening size. **Can be noticed that pressure decrease is quicker as the opening is wider.** The gap between simulations gets more important as time goes by. This result was expected as visible in reference [3] . Oscillations impact similarly wall 6 and 4.

3.4 section's outcomes

The validation process has been successful on the 3D mesh and 2D simulations' results are in accordance with references. These observations are positive and give credibility to mesh's performance and chosen FLUENT parameters.

The study 'global versus local measurement" shows smoother results via wall measurements and represent correctly the cabin decompression. No major discrepancies appear

between walls except walls 6 and 4 which suffer from oscillatory behaviors. Local measurements at points generates more oscillations. Nevertheless they highlight other phenomena such as pressure peaks and pressure differential (which can be used for structural analysis).

Refinement impacts pressure results in term of tendency, oscillations and pressure peak. Results' gap between meshes differ between coarse/medium and medium/fine. The refinement study is continued on Charles's section where a Grid Convergence Index is performed.

4 Results Charles

4.1 Mesh choice and convergence study

4.1.1 Mesh refinement and results

The objective of this part is to determine which mesh refinement is suitable to run basic simulations with Fluent. All the work presented in this section is based on ICEM structured meshes whose walls definition and nomenclature is explained in Figure 1a. The mesh needs to be a good balance between satisfying results and reasonable computational time. In order to choose a suitable mesh to run various simulations, 3 different base meshes have been created using ICEM following the previously defined geometry. Each mesh have a different number of cells and nodes leading to 3 levels of mesh refinement. This part focus on establishing an ideal mesh, not on analysing the physical phenomenons.

The Table 3 summarize the characteristics of the coarse, medium and fine mesh.

Mesh	Number of nodes	Number of cells	Type	Refinement ratio
Coarse	8013	6956	Structured	/
Medium	32225	28310	Structured	4.02
Fine	144409	129256	Structured	4.48

Table 3: Initial meshing definition

The Fluent setup is done with previously presented data which correspond to a flight at 35000ft altitude in nominal conditions. The parameters are also detailed in the Table 6. For the convergence study, the Operating pressure is set at 101325 Pa which is Fluent default configuration. The Figure 19 hereafter shows a plot of the Average Pressure results using the Coarse, Medium and Fine mesh

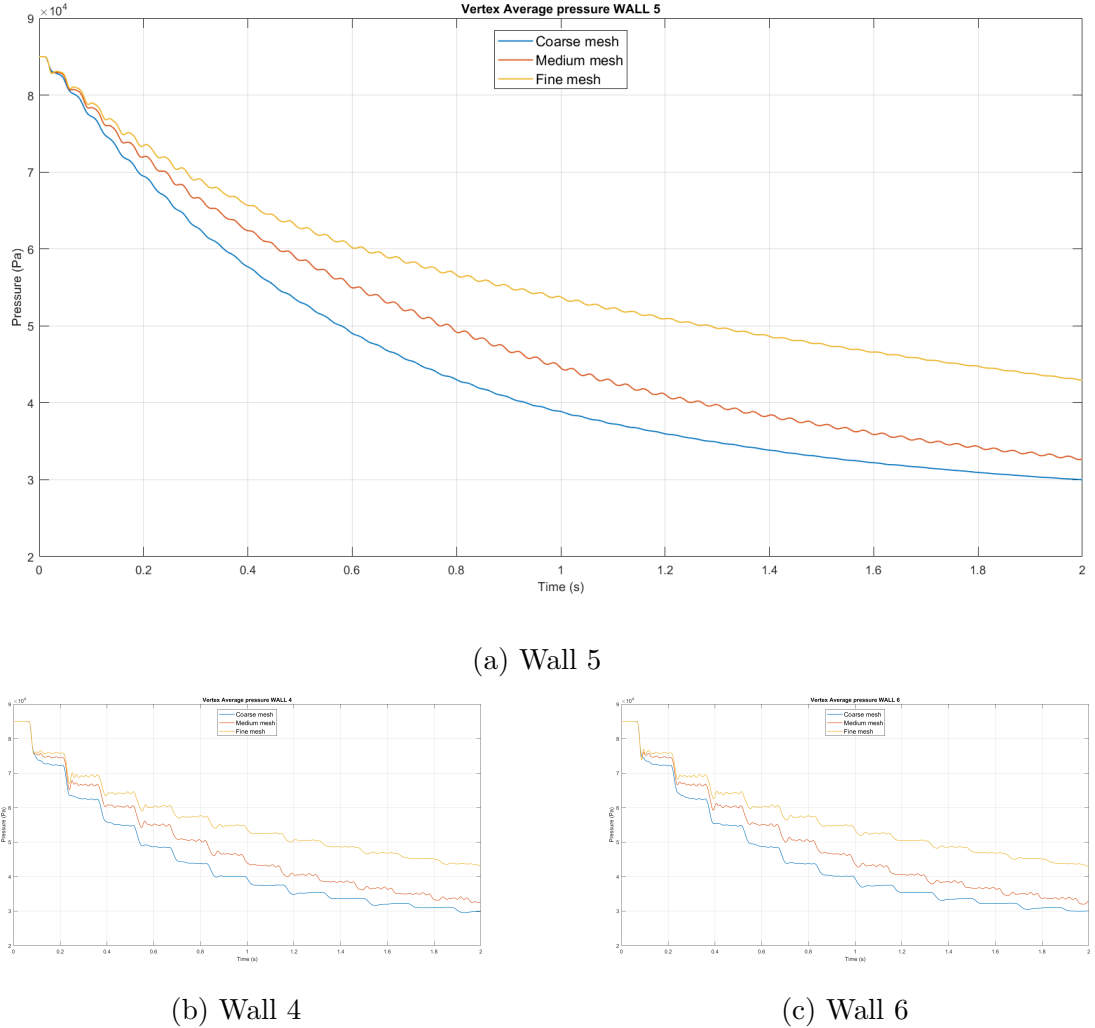


Figure 19: Average pressure results for different mesh refinements

On the Figure 19, the Vertex Average pressure of the wall 5 which is the wall in front of the opening, the wall 4 and wall 6 which are the front and back wall of the cabin are initially at the cabin pressure of 85000Pa. Then, on each wall the pressure is smoothly decreasing. We can remark that the Results are totally consistent and math the Validation and Verification done by Giorgio.

Visually, we can notice that on the very first time steps, the gap between the Coarse, Medium and Fine mesh is really small. However, as time goes by, the gap between the meshes is globally increasing. This observation is true for all the walls of the cabin. For this reason, it is useful to study how the mesh converges at different time steps where there is significantly different gaps. Qualitatively, we can choose 3 points which are representative of the curves: t=0.1s, t=0.5s and t=2s.

4.1.2 Relative differences

Firstly, the relative differences criteria is a simple but interesting parameter to study. The relative differences are computed at the announced time steps with the formula 2

$$\delta_{relative(\%)} = \frac{|U_1 - U_2|}{U_2} * 100. \quad (2)$$

The error is computed with 2 between mesh 1 (coarse) and mesh 2 (medium) and between mesh 2 and mesh 3 (fine). δ_{12} is the relative error between mesh 1 and 2 while δ_{23} is the relative error between mesh 2 and 3.

The Table 4 hereafter gives the relative error for the different time steps for wall 4 and wall 5.

$\delta_{relative(\%)}$	Wall 4		Wall 5	
	δ_{12}	δ_{23}	δ_{12}	δ_{23}
t=0.1s	1.6682	0.8805	1.4528	0.7665
t=0.5s	8.7776	6.3476	9.2642	6.6565
t=2s	7.6353	24.5129	8.2675	23.7972

Table 4: Relative error between the meshes

This data is plotted on Figure 20 in order to be commented.

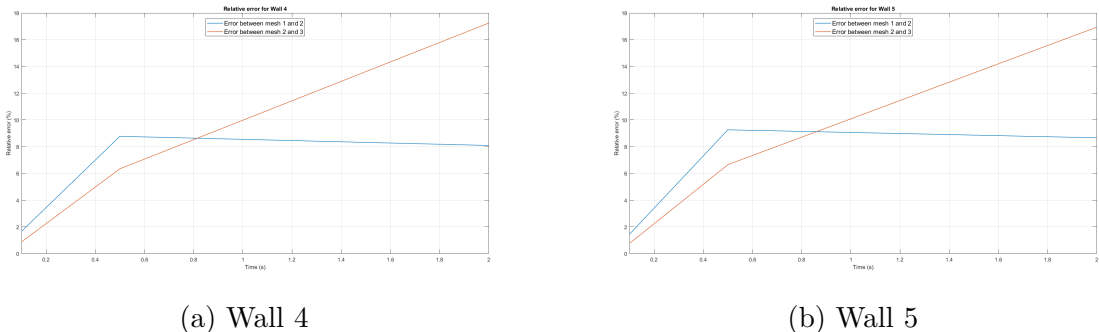


Figure 20: Evolution of the relative error between coarse, medium and fine meshes

We can observe that the behavior of the relative error between the meshes is similar for both the wall 4 and 5, values only change slightly (only few %). If we compare δ_{12} for the different time step zones, it is very small at $t=0.1s$, approximately 1.45%, it then increases to approximately 9% at $t=0.5s$ and just slightly decreases of about 1% until last time step $t=2s$. However, it is not the same for δ_{23} . At $t=0.1s$, the error is very small, approximately 0.8%, it also increases slightly to 6% at $t=0.5s$ but at $t=2s$, the difference between mesh 2 and 3 become considerably bigger, differences of 25% are reached. These observations show that the discrepancies between all the 3 meshes are very small for the first time steps, then discrepancies become slightly bigger for the next times step. For

$t=2s$, which is the final time step of this simulation, the relative difference is contained at the same level between coarse and medium mesh. On the contrary, between medium and fine mesh, the relative difference become very big for $t=2s$. This means the finer mesh change the result significantly after a time of approximately 1s. At the opposite, the refinement does not change notably the pressure results for the very first time steps, which are assumed to be the most interesting as part of this project.

Therefore, the medium mesh will be used in the next subsection as it is considered to produce sufficiently accurate results with a reasonable computational time. Computing the medium mesh, one simulation takes approximately 3 hours, but with the fine mesh, the same simulation takes around 7 hours, which is not acceptable for this study as many simulations need to be launched.

4.1.3 Grid Convergence Index

In a second part, the GCI will be calculated for our coarse, medium and fine meshes. The Grid Convergence Index (GCI) is a relevant tool in order to study the effects of the mesh refinement.

The GCI method is given by [5]. It "indicates an error band on how far the solution is from the asymptotic value" [5]. The GCI indicates if the solution could be more accurate if the grid is refined again. Here the Vertex Average pressure result will be studied on the wall 4,5,6.

With f_1, f_2, f_3 the result obtained with coarse, medium and fine mesh results respectively, the order of convergence p is defined as

$$p = \frac{\ln(\frac{f_3-f_2}{f_2-f_1})}{\ln(r)}. \quad (3)$$

Ideally, the refinement ratio should be an integer and be the same for all of the refinement.

$$GCI = \frac{F_s |\epsilon|}{r^p - 1} \quad (4)$$

F_s is the security factor, 1.25 is recommended for 3 or more meshes.

We should have:

$$Ratio = \frac{GCI_{23}}{r^p GCI_{12}} \approx 1 \quad (5)$$

The Table 5 shows the convergence ratios at different time steps ($t=0.1s$, $t=0.5s$, $t=2s$).

Ratio	$t=0.1s$	$t=0.5s$	$t=2s$
Wall 4	0.279	0.544	0.924
Wall 5	0.279	0.538	0.917
Wall 6	0.090	0.551	0.912

Table 5: Convergence ratio

These results confirm the observation of the previous part. For the first time steps $t=0.1s$ and $t=0.5s$, the Ratios are low and far away from 1 (between approximately 0.1 and 0.55). However, at $t=2s$ the Ratio is closer to 1 which means there is a convergence between the coarse, medium and fine meshes. As seen previously, this observation is valid for wall 4 and wall 5, but also wall 6 which is the other side of the cabin.

4.2 Influence of the altitude on the decompression

Among all the flight parameters, the influence of the altitude on the decompression is an important and interesting parameter to study for a pressurised airplane. Indeed, a commercial airliner like the A350 fly through very different external conditions, a plane can climb from sea level to cruise altitude of 35000ft or greater. The cabin of the plane is always pressurised through all the phases of the flight, from takeoff to landing. It also happens that the plane stays at lower than cruise level during departure, arrival or holding pattern procedure. For these reasons, it is important to understand which effects a decompression can have on the aircraft at various altitudes.

In this study, we will firstly compute the pressure on the cabin walls at a cruise altitude of 35000ft which is the core of this problem. Secondly, we will study what happen at other altitudes with the cabin always pressurised in the same conditions. The same meshes as previously are used. Table 6 and 7 summarize the conditions used (ISA conditions) based on altitude. On every simulation, we assume the plane fly at constant Mach number at every altitudes, which is a small simplification of a classic flight profile. This set up allows to compare accurately the true effects of the altitude parameter on a decompression. The flow is then fixed to M0.82 which corresponds to a typical cruise speed.

#	Altitude (ft)	P (Pa)	T (K)	M	Velocity ($m.s^{-1}$)
1	15000	57182.0	258.432	0.82	264.1591
2	25000	37600.9	238.620	0.82	253.8317
3	35000	23842.3	218.808	0.82	243.0659

Table 6: Outside air conditions

For the cabin, we retained parameters which are as close as possible from the reality. We assume that the conditions are constant, which is not exactly the same in a commercial

airplane but it was complicated to simulate the evolution of the cabin parameters of an airplane during a flight. Conditions are always the following:

#	Altitude (ft)	P (Pa)	T (K)	M	Velocity ($m.s^{-1}$)
ALL	5000	85000	300	0	0

Table 7: Cabin air conditions

Results are computed on the previously studied walls 3,4,5,6,7 which are the front and rear cabin wall as well as the wall in front of the door.

Hereafter, Figure 21 shows these results

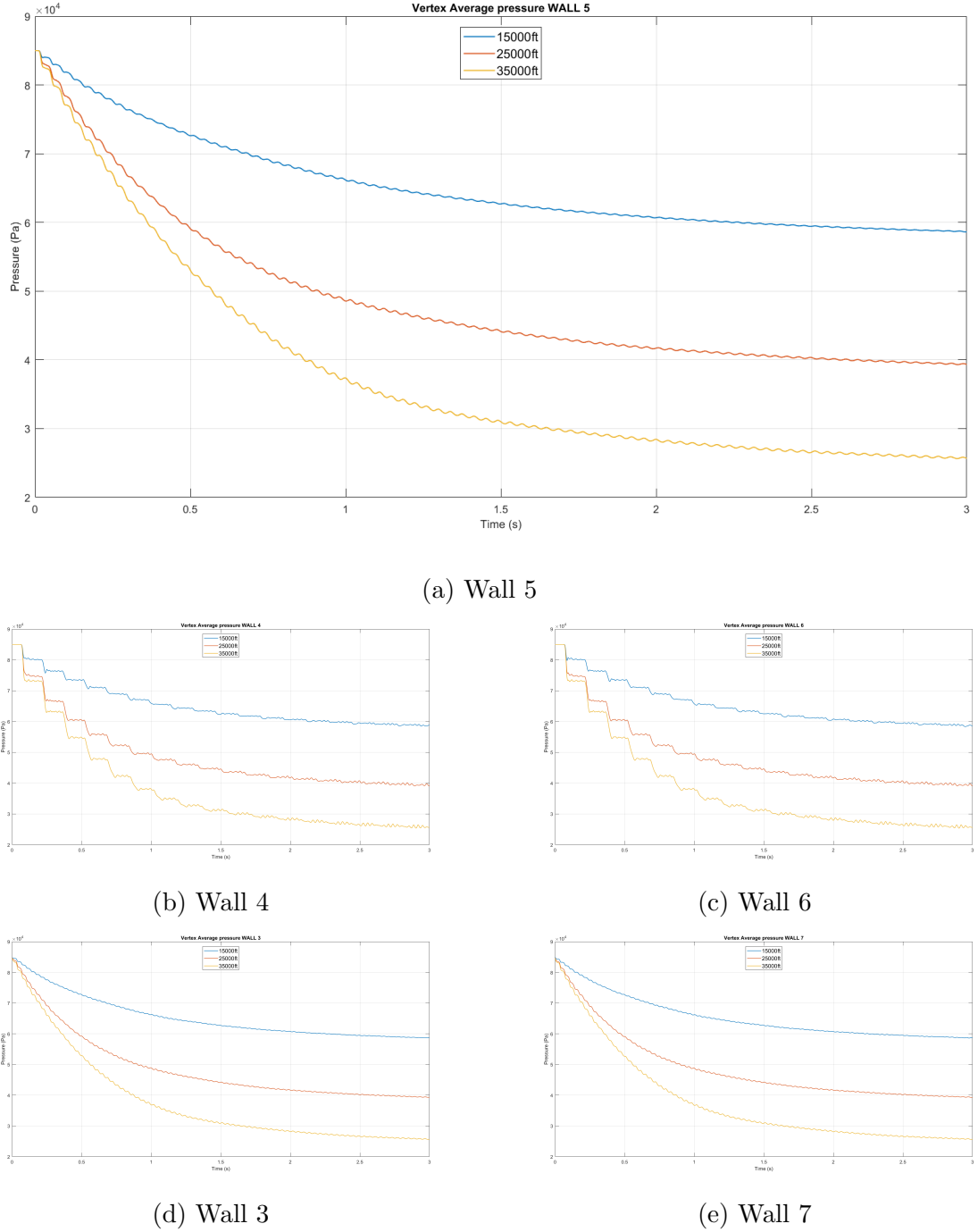


Figure 21: Vertex Average pressure results for different altitudes

Qualitatively, we notice that the evolution of the pressure always follows the same behavior. The more the altitude is low, the slowest the decompression is. We can investigate the Lost of pressure on the Wall 5 on the cabin on the Figure 22.

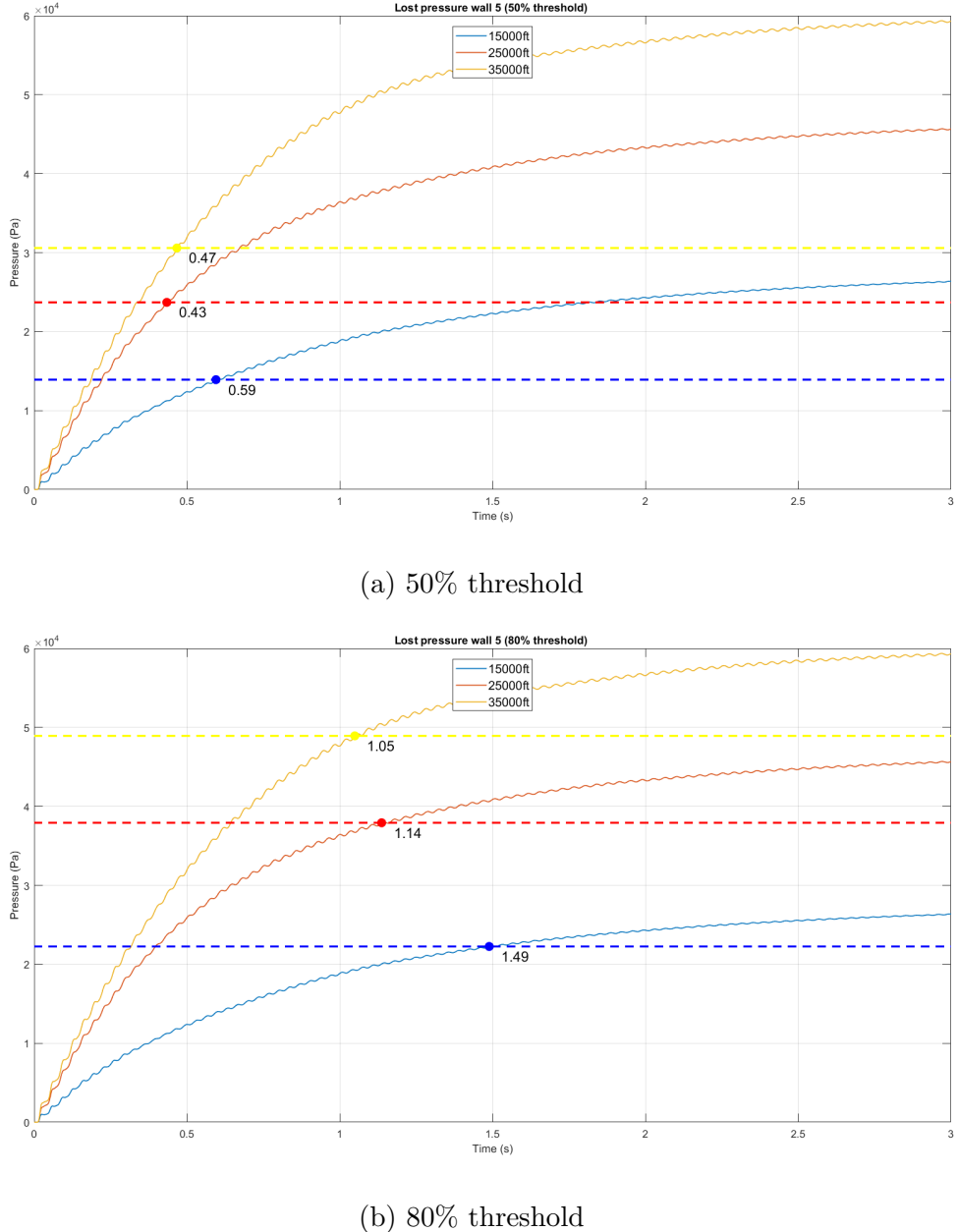


Figure 22: Lost of Vertex Average pressure on Wall 5 with thresholds

As the cabin pressure remains constant at $P_{cabin} = 85000$ Pa, the difference of pressure between the cabin and the exterior is defined here as $\Delta P = P_{cabin} - P_{exterior}$. Hence, within our test cases we have

- $\Delta P_{15000ft} = 85000 - 57182 = 27818$ Pa
- $\Delta P_{25000ft} = 85000 - 37600.9 = 47399$ Pa
- $\Delta P_{35000ft} = 85000 - 23842.3 = 61158$ Pa

On Figure 22a, the dashed line shows the 50% threshold of the difference of $\Delta P_{15000ft}$, $\Delta P_{25000ft}$ and $\Delta P_{35000ft}$ respectively. The time to reach the 50% threshold is marked on

the Figure, for 15000ft, it takes 0.59s, for 25000ft 0.43s and for 35000ft 0.47s. This means that the relative differences between the 15000ft and 25000ft altitudes are $\approx 36\%$ while it is only 9% between 25000ft and 35000ft. On the Figure 22b this is the same graph but with a 80% threshold. For 15000ft, it takes 1.49s, for 25000ft 1.14s and for 35000ft 1.05s. For this threshold, the relative differences are $\approx 30\%$ between 15000 and 25000ft and 8% between 25000ft and 35000ft. We can notice that the behavior is the same for the 2 threshold studied. Proportionally to the difference of pressure, the pressure takes a longer time to balance as the ΔP become smaller, which is in this case equivalent to a lower altitude of the plane. There is a small exception for the 50% threshold of 25000ft altitude, however this does not exist with slightly different conditions. These observations mean that the more the plane is flying low, the more the decompression is slow. The same phenomena is observed on the other walls of the cabin (WALL 4 and WALL 6) and the results is then not detailed. On these cases, there is no evidence of over pressure on the walls which can be dangerous for the structural integrity of the aircraft.

4.2.1 Investigation of Average and Maximum Vertex pressure

As Fluent allow to compute different expression of the pressure, it is also interesting to investigate about the Vertex Maximum pressure and compare it with Vertex Average Pressure. In Fluent, the vertex average of a variable on a surface is computed by dividing the summation of the vertex values of the variable by the total number of vertices. The Vertex maximum of a variable on a surface is the maximum vertex value of the selected variable on the surface [2].

On Figure 23 hereafter, the Average and Maximum Vertex pressure are compared on the Wall 4,5,6 with the 35000ft exterior conditions described above.

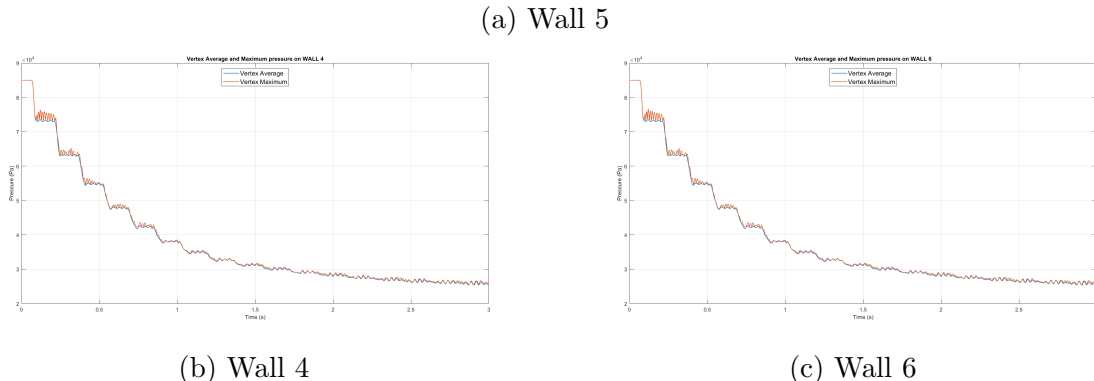


Figure 23: Vertex Average and Maximum pressure on Wall 4,5,6

The plot shows there is no physical significant differences between the results on all these cabin walls. Vertex Maximum shows that the pressure drop is slightly less regular, however, the simulation does not show any pressure peaks or irregular behavior of the pressure.

4.2.2 Investigation of the pressure on door frame and exterior effects

In this section, simulation conditions #1, #2, #3 of Table 6 are computed, this corresponds to a flying altitude of 15000, 25000 and 35000ft. The Vertex Average pressure on WALL 2 and WALL 8 is computed. These 2 walls correspond to the door frame of the cabin (Figure 1a). These 2 small walls are also interesting to compute for structural resistance purposes.

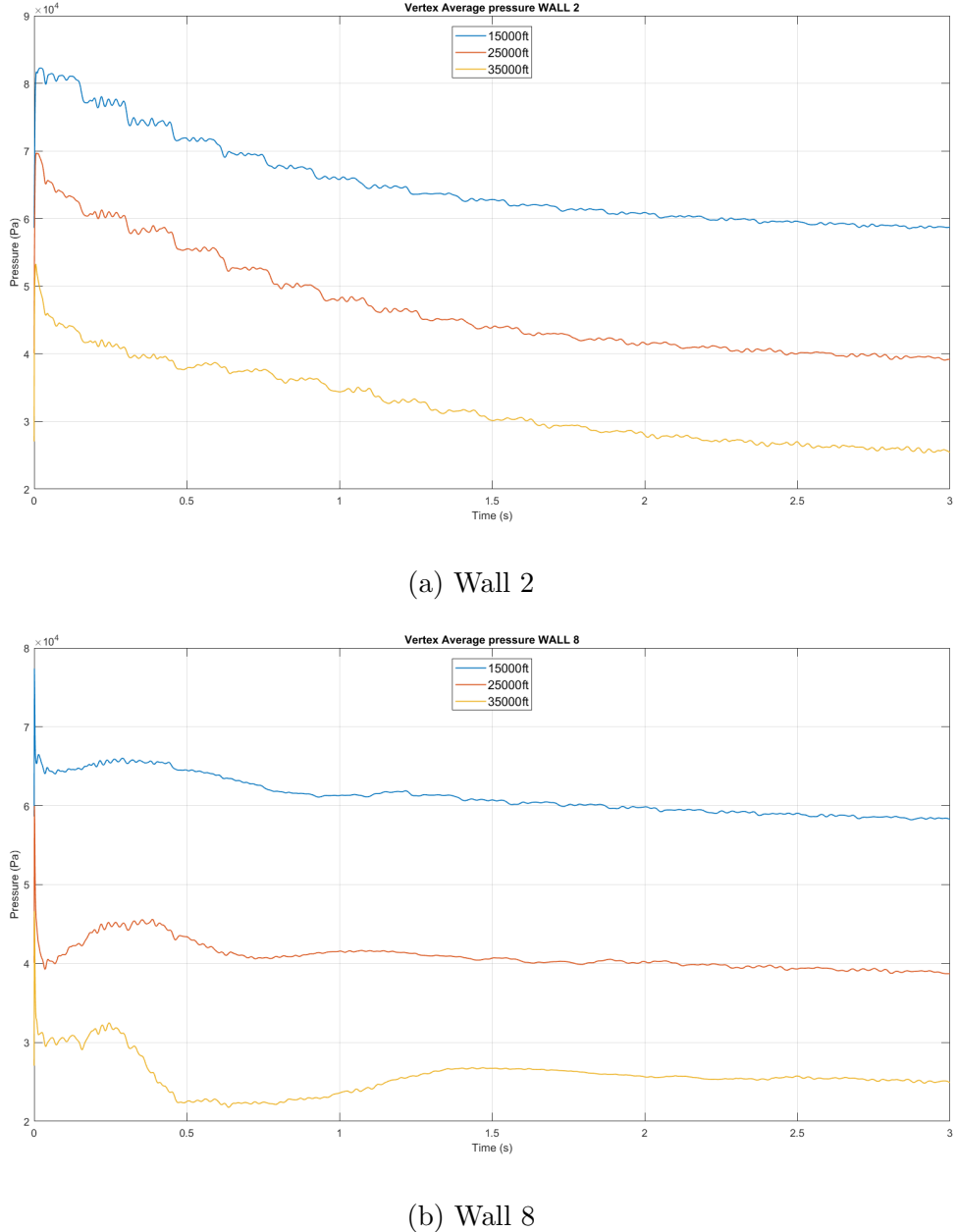


Figure 24: Vertex Average pressure on door frame Walls 2,8

On these 2 walls, we can remark visually that the behavior of the pressure is slightly different than on the cabin walls. Globally, the pressure on the door frame walls decreases over time. However, at the very beginning of the time after the detachment of the door,

a pressure peak is observable on the Wall 8. The maximum value reached is ≈ 77000 Pa. This is reached with test case #3, with the highest cruising altitude. This value is negligible as it is lower than the normal cabin pressure. However it is apparent that this value should be taken into consideration regarding the impact of this pressure on the door frame area.

Hereafter, the Pressure contours are plotted for the test case #3 which corresponds to the 35000ft flying altitude. The Figure 25 highlights the transitional pressure balancing phase which is plotted for the cabin walls in the previous sections.

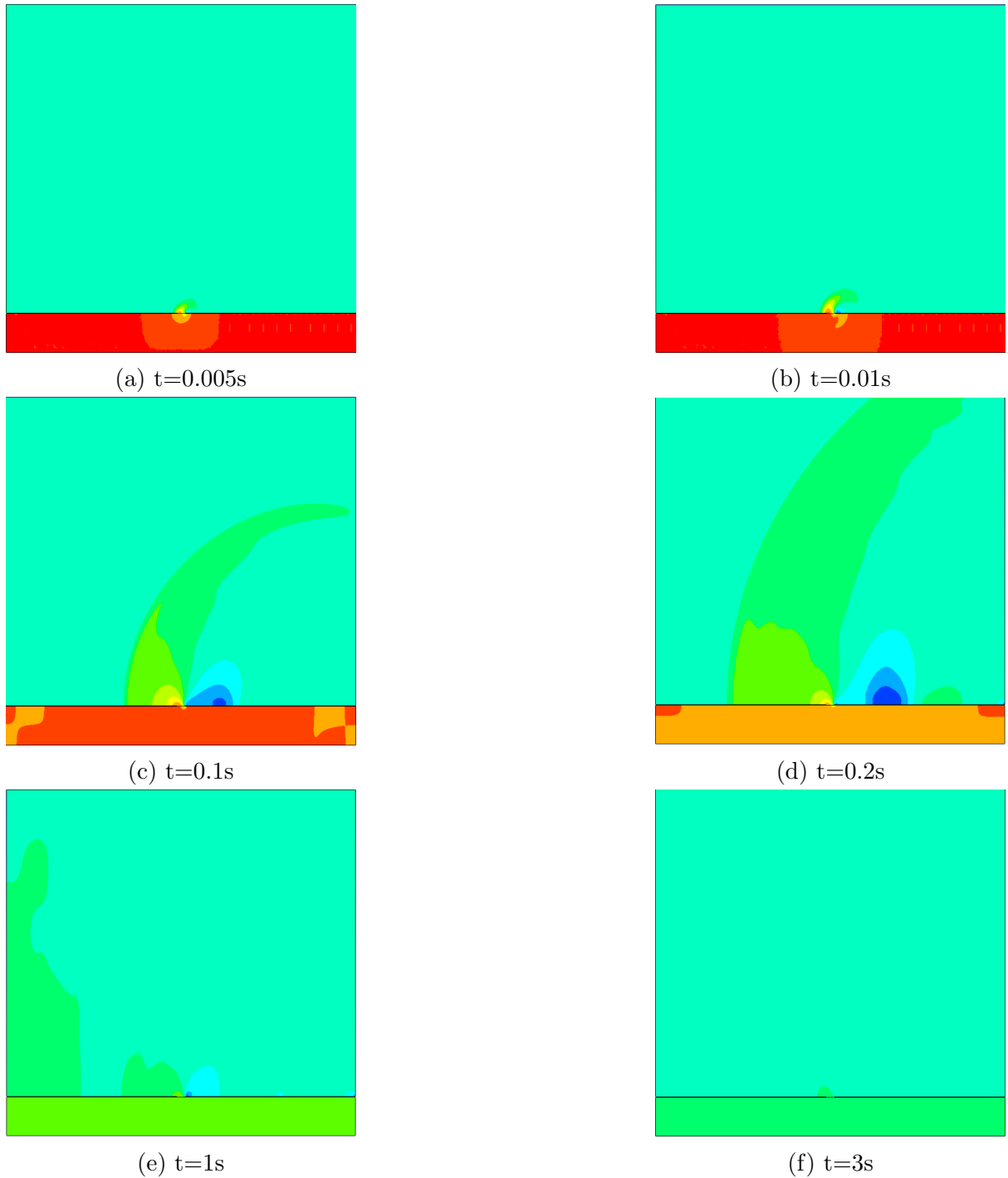


Figure 25: Overall contour of Pressure

As before, the airflow is going from left to right on this simulation. On Figure 25a, straight after the loss of the door, the pressure on cabin wall near the door decreases progressively. On Figure 25b, we can see that an high pressure zone appears before the door while the cabin pressure is decreasing smoothly. Figure 25c shows that a zone of low pressure appears after the door on the exterior of the fuselage, the effects continue to spread on the Figure 25d but slightly moves backward. On the Figure 25e, the outside effects disappeared. The cabin pressure continue to decrease smoothly to reach a very

stable situation as we can see on Figure 25f. On the Figure 26a hereafter we can see the Vertex Average pressure for the Wall 1 and Wall 9. In contrary to the contours, the results are presented for the test cases #1,#2,#3. The slight pressure increase is clearly distinguishable between $t=0\text{s}$ and $t=0.1\text{s}$ as seen previously. After $t=1\text{s}$ or 1.5s , the effects slowly disappear and the pressure stabilise to exterior air conditions (Table 6). At the opposite, the Figure 26b shows the slight drop of pressure which have a similar behavior in the same time. The drop and over pressure effects are most important when the altitude of the plane is high, which means the external air pressure is less important (test case #3).

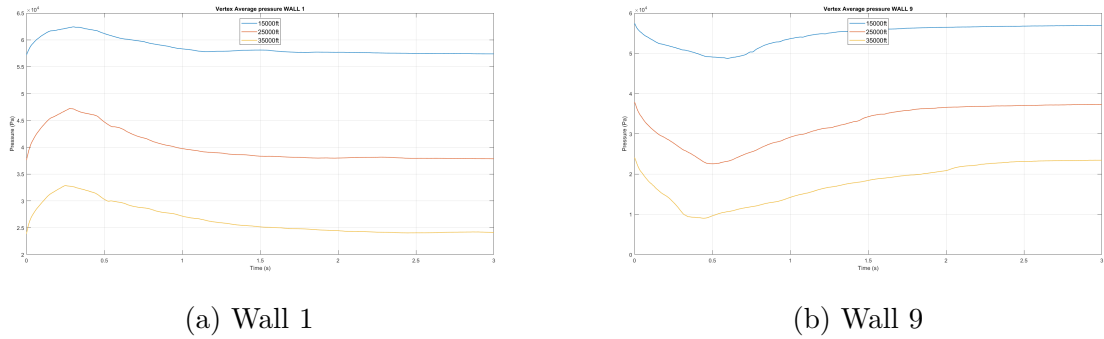


Figure 26: Vertex Average pressure on the exterior fuselage

To conclude, the effects of a decompression on the cabin walls is a smooth loss of pressure as presented before. However, a small peak of high pressure can appears on one of the door frame, it is reaching 77000Pa in the case of a decompression at 15000ft. The more the outside pressure is high, the more this peak of pressure seems to be important. On the fuselage, a phenomena of under pressure appears straight after the door. If in this part, no "dangerous" peak of pressure appeared inside the cabin, it is not the case for the door frame zone, where the slight over pressure is interesting. Secondly, the under pressure which appears on the fuselage could have dangerous effects as the cabin pressure is still high when it happens, as we can see on Figure 25d. This problem is treated in more depth in Sévan's section.

5 Results Thibault

In order to pursue this parametric study, the choice of using different size of doors that is possible to find in a commercial aircraft. To compare the influence of the size of a door, it has been decided to fix a unique physical model. The inviscid model used before is the one chosen, and the simulation is computed over 3s with a time step of 0.01s. The mesh chosen for the simulation is the medium mesh.

In the case of this study, four different types of doors are tested : The A-350 door used previously (1.26m), the Type I door (1,85 m x 0,81 m) present on the range of Airbus airplane 138 to 321, the type III emergency door (1,02 m x 0,51 m) fitted on the A-320 and the type C emergency door (1,52 m x 0,76 m) situated both at the front and the back of the A-321. Here again, the idea was to evaluate the pressure on the structure, and be sure that the forces applied on the walls during the rapid decompression wouldn't

put in danger the integrity of the civil airliner.

As expected, the global behavior of the pressure inside the cabin, in particular on the interior walls, correspond to a decrease (fig 5a to fig 5e). First, if we compare the evolution of the average of the static pressure applied on the walls, two different types of behavior are noticeable. The walls 3,5 and 7 (respectively fig 5a,5c and 5e) have small oscillations during the first 0.35s of the rapid decompression and then the decrease of the average temperature become linear. However, for the walls 4 and 6 (fig 5b and fig 5d), corresponding to the wall at the front of the aircraft and at the back, these oscillations are present until 3s(the end of the simulation).

Also, the peak of pressure that could be expected at the very beginning of the simulation is not present for each of the simulations. In term of quantitative analyse, obviously the smaller is the size of the door, the slower the pressure is decreasing. Indeed, after 3s, the average pressure for the type III doors is about 7.4 kPa, and this type is the smallest type of door in this study. Come after the type C and the type I, respectively, with an average pressure of 7.1 kPa and 7.05 kPa. Finally, for the largest type of door, the A-350 door, the average pressure on the walls after 3s is about 6.6 kPa (fig 5a to fig 5e).

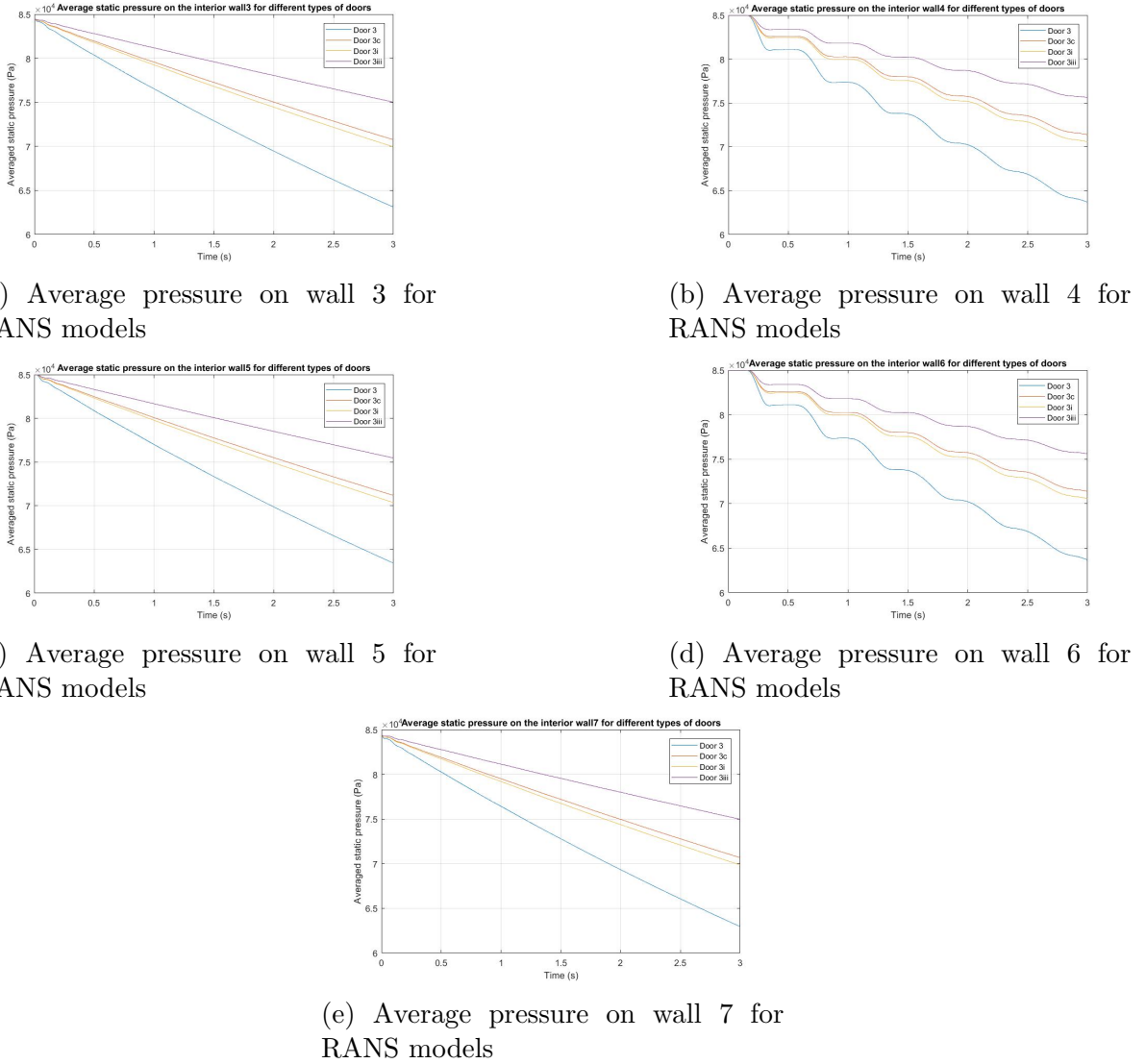


Figure 27: Study on RANS models

The oscillation present for the average pressure could be the result of peaks of pressure along the wall, and intense peaks could damage the aircraft structure. Indeed, a second analyse is necessary. This analyse is focusing on the maximum pressure applied on each wall during the decompression (fig 6a to 6e).

The first remark, is that for every graphics the same global decrease is observable. The main difference lies in the oscillations. Now, for every wall, the decrease oscillate until the end of the simulation (3s). Looking closely to those curves, two different types of oscillation are noticeable. The frequency of the oscillation for the walls 4 and 6 is about 2Hz (fig 6b and 6d), and the frequency of the oscillation for the walls 3,5 and 7 is 4Hz (fig 6a,6c and 6e), that is to say, twice the frequency for the walls 4 and 6.

The second remark is about the peak of pressure expected. Again, this peak is not present at the very beginning of the decompression, and even further, this analysis shows that in none of the curves, the oscillation of the average pressure is due to peaks of pressure. Indeed, the curves describing the behavior of the maximum pressure only illustrate small

variations in the decrease of the pressure but not any strong peaks of pressure. Finally, in terms of quantitative analyse the same conclusion as the previous analyse can be made. The smaller the door is the slower the pressure will decrease. Indeed the faster decrease is for the A-350 door with a maximum pressure around 6.5 kPa after 3s. Then come the type I with a maximum pressure of 7.1 kPa. The third most rapid pressure decrease is for the type C with a maximum pressure estimated around 7.15 kPa, and finally the type III, the smaller type of emergency door has a maximum pressure after 3s around 7.45 kPa.

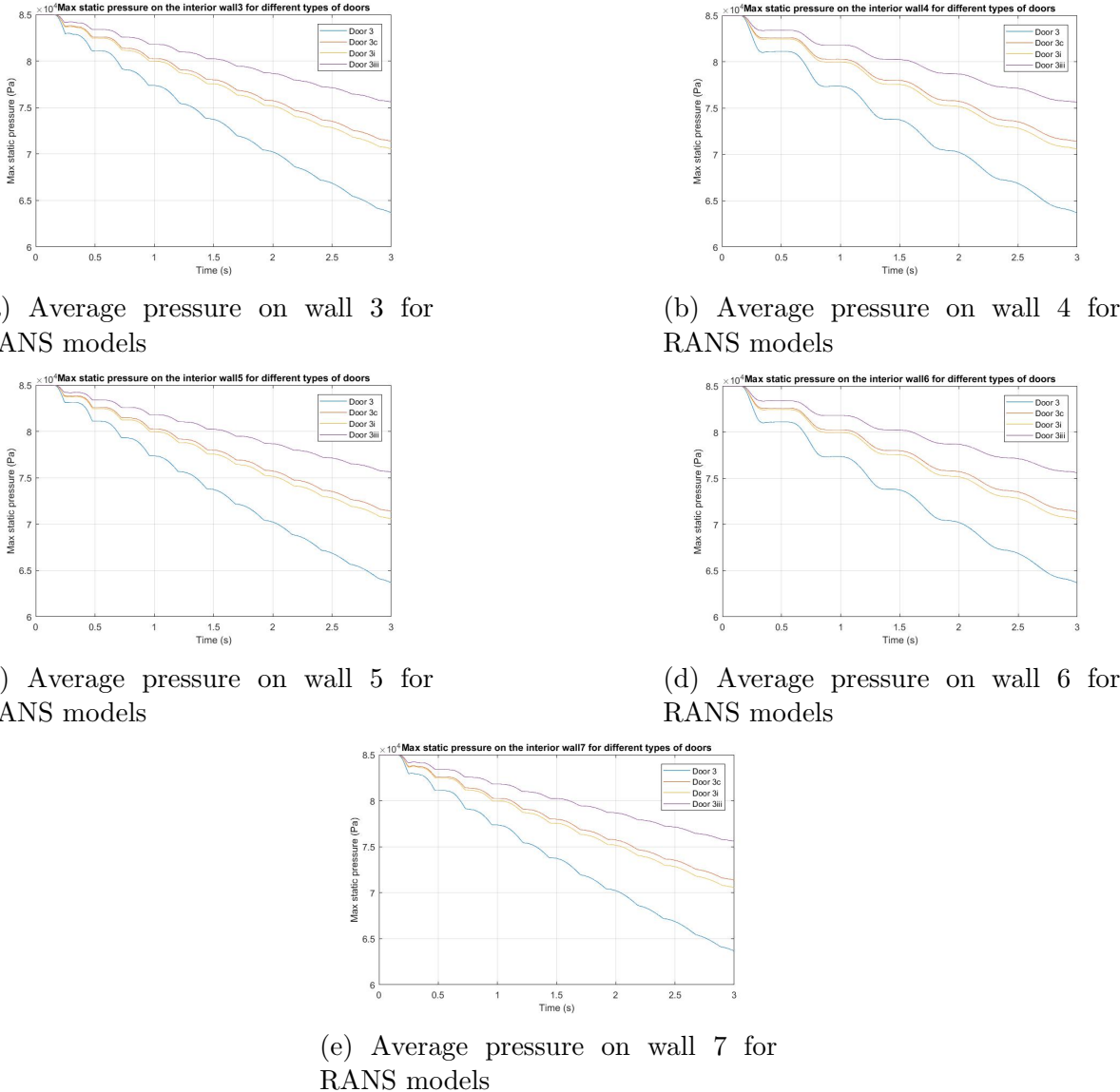


Figure 28: Study on RANS models

So, as a conclusion the size of the door influence obviously the decrease of the pressure applied on the wall. The smaller the door is, the slower the decrease will be. None peaks of pressure appeared during those simulations. It means that the structure of the aircraft is not in danger when a rapid decompression occurred. However, it is relevant to notice that oscillations are created during the decrease of the pressure. To pursue this analysis

more in depth, a study in 3D could bring more details about the behavior of the pressure with different types of doors, as well as studying if the position of the door along the aircraft influence the decrease of the pressure. It would be also interesting to study if the oscillations during the decrease of the pressures could create vibrations that could put in danger the integrity of the structure of the aircraft.

6 Results Rafi

As the document of the Airbus shows (The A350 Aircraft Characteristics), the A350-900 contain another type of opening. In the flowing simulations, the cargo compartments opening are ran and investigated. In the first place, the geometry was changed as represented in the (figure 29). The cargo opening are positioned in the front of the cabin figure(a) and in the back of the cabin figure(b). According to the Airbus document of the A350 characteristics, the front cargo opening size length is 2910 mm where the backward cargo opening measures 2850 mm. Moreover, each opening are positioned in the real location compared to the cabin. Similar to the (figure 1), the cabin and far-field dimensions remains the same.

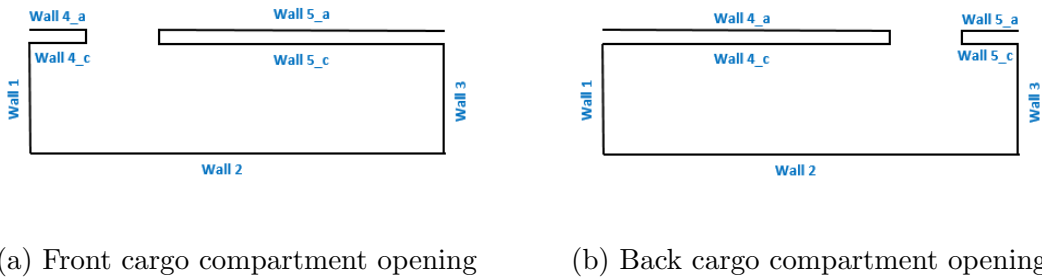


Figure 29: 2D Geometry and name of the walls of the two cargo compartment

The Meshes used in these simulations represent (17251 nodes) and it were performed with the software ANSYS Workbench. Furthermore, all the setup used for the software FLUENT are the same mentioned previously. The Far-field pressure is equal to 85000 Pascal where the cabin pressure is equal to 25000 Pascal. The Far-field temperature is equal to 220-kelvin while the cabin temperature is equal to 293-kelvin. Meanwhile, the velocity of the Far-field is equal to 243.7271 m/s in the x direction and it is equal to zero inside of the aircraft cabin.

The following figures presents the pressure value during 3 seconds. Each figure illustrate only one wall for both of the geometry. The front curve (in red) present the front cargo opening where the Back curve represent the backward cargo opening (in black).

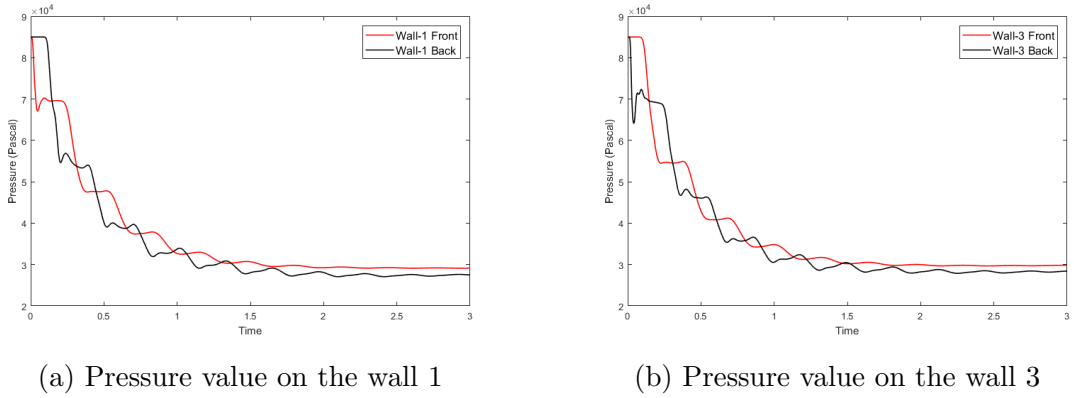


Figure 30: Pressure curves on the front and back cabin walls

On the first glance, the (figure 30) shows a very similar behaviors. The Wall 1 and 3 represent both ends of the cabin, the front and the back respectively. Depending on the location of the cargo opening, the two curves behave inversely. As an example, the (figure 30(a)) shows the wall 1 with the back cargo opening remaining the pressure at 85000 Pascal in the first fractions of seconds where this behavior is the same for the wall 3 with the front cargo opening. In addition, the back opening shows an oscillatory behavior that can be caused by the flow direction (left to right). Besides, it is obvious on both figures that the pressure of the walls drop to a stability point around 1.5 seconds. However, by the time goes by, the front opening cargo shows a higher pressure value and neither of the walls or the opening cargo locations shows a stability pressure equal to the Far-field pressure at 25000 Pascal. Generally speaking, both walls shows a stairs phenomenon with a big drops in the pressure when the time goes by.

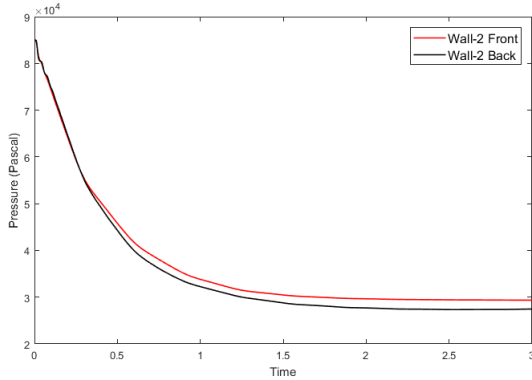


Figure 31: Pressure curve on the side cabin wall (Wall 2)

Next, the (figure 31) illustrate the pressure values at the wall 2 for the two cargo opening locations. As it is noticed graphically, both of the pressure curves decreases smoothly about 55000 Pascal between 0 to 1.5 seconds. This speed of decompression demonstrate a strong behavior in very small amount of time that can be the cause of the aircraft damages. Once again, the Front opening cargo compartment shows more time to reach the far-field pressure 25000 Pascal.

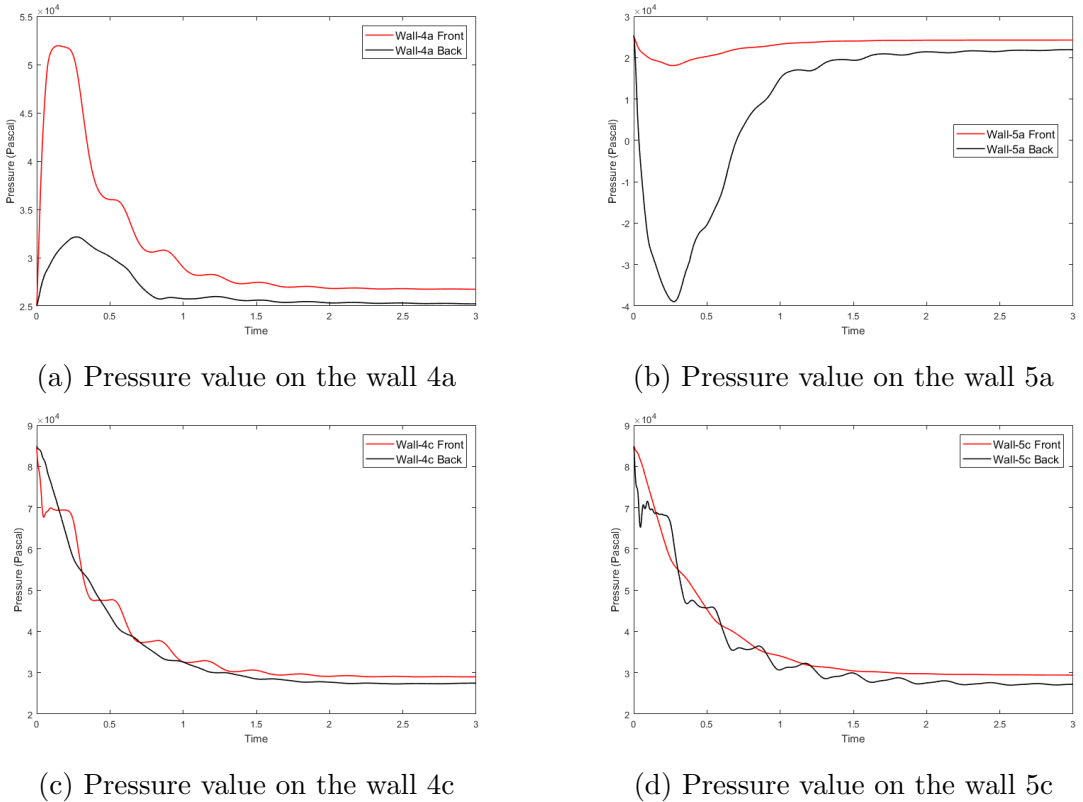


Figure 32: Pressure curves on the Walls next to the opening zone

Subsequently the (figure 32) present four different walls inside and outside of the cabin. Theoretically, the walls 4a and 4c represent the same wall, likewise for the walls 5a and 5c. It is more interesting in this study to separate both walls and investigate closely each pressure curve evolution. In the first place, by looking at the Front cargo opening (red curves), the wall 4c shows once again a stairs behavior with pressure drops. In the meantime, the curve on the wall 5c look smoother by decreasing from 85000 to around 25000 Pascal. Meanwhile, the wall 4a which is located outside of the cabin shows a very interesting behavior by increasing from 25000 to reach almost 55000 Pascal and then decreasing slowly within 1.5 seconds. In contrast, the pressure on the wall 5a shows a small decompression before rising up again to reach the Far-field pressure at 25000 pascal.

Secondly, the back cargo opening (black curves) shows more and less the same behaviors. In the first hand, the Walls 4c and 5c are showing the same pace of the front cargo opening. One difference noticed between the two walls, the 4c wall shows a smooth decreasing curve while the 5c drop off by several stages. In the other hand, the curve on the wall 5a shows a pressure drop of almost 66000 Pascal to reach - 40000 and increase again within 1.5 seconds. This zone remain to be important where vortices appears right after the opening cargo compartment. As a matter of fact, the (figure 33) shows clearly the decompression area backward outside of the opening zone.

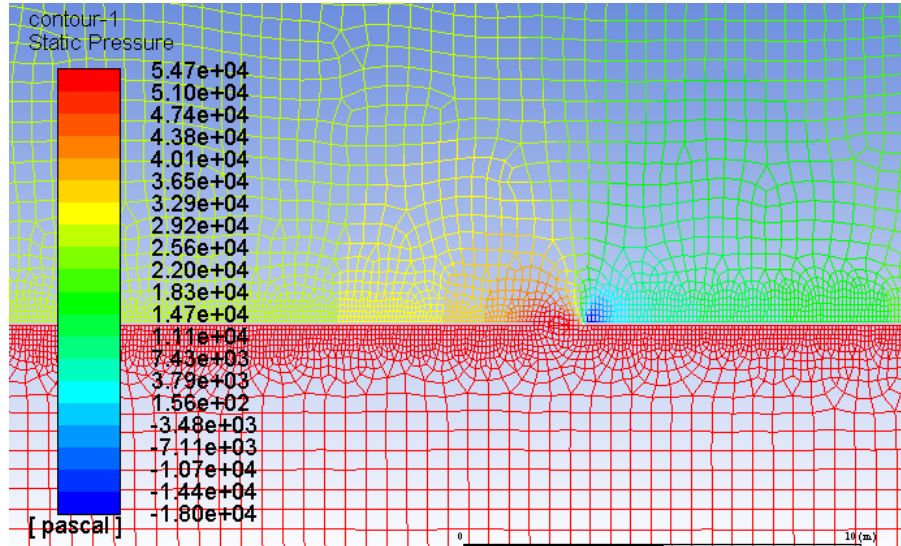


Figure 33: Different pressure zones next to the cargo opening compartment

These results can be one of the reasons for the fuselage damages, where the inside pressure on the wall 5c is 85000 Pascal, while the outside pressure on the wall 5a drop significantly. This hypothesis can be validated if a pressure peak appears on the inside cabin walls. Unfortunately, no peaks are detected around the opening zones.

7 Results Sévan

7.1 Parameters and their impacts

After having investigated the impact of mesh refinements, several accurate simulations have been performed in order to study the pressure behaviour on different zones of the cabin. This part will try to figure out the impact of different parameters on the pressure evolution. Those parameters are the velocity through the Mach number, and the opening size. For this investigation, coarser meshes and a bigger time step have been used in order to reduce the computational time, considering the number of simulations. The cases of this study are all summarised in the following table:

simulation Cases		
Cases	Opening size	Mach number
case 1	0.3m	0.5
case 2	0.3m	0.72
case 3	0.3m	0.82
case 4	1.27m	0.5
case 5	1.27m	0.72
case 6	1.27m	0.82
case 7	3m	0.5
case 8	3m	0.72
case 9	3m	0.82

In this part, all the meshes have been built via the meshing software of ANSIS

workbench, the abbreviations "wall1", "wall2"...ect are summarised Figure 1b in the methodology part. The Figure 34 shows the time evolution of the pressure averaged on the Wall1 and Wall3. Those walls are equidistant from the opening in order to see if the outside flow direction can have an impact on the pressure, far from the opening, to a the wall1 at the left, the the wall3 at the right.

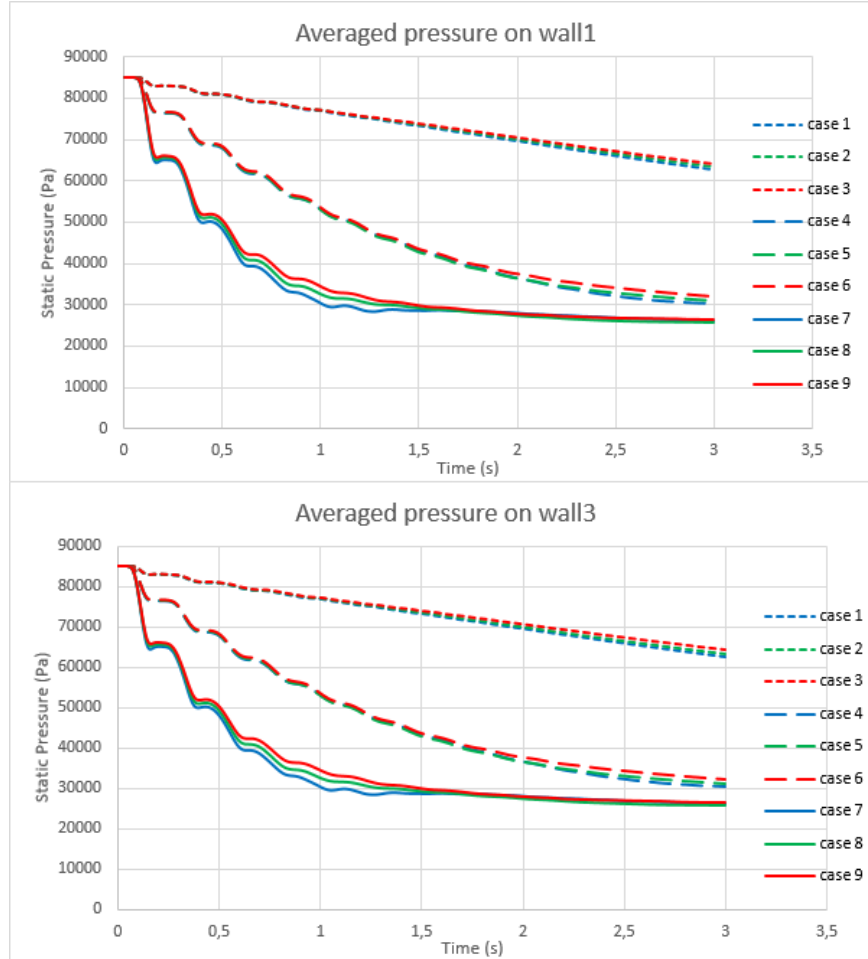


Figure 34: pressure evolution for all the cases

As those curves as very similar to each-others, the impact of the outside flow direction on the pressure evolution, far from the opening, is not significant for an centred opening. Regarding the evolution itself, as already observed, the depressurisation is faster for a larger opening or for a lower Mach number. As observed in the section 4.2, a lower altitude that implies a lower difference between the pressure inside and outside the cabin will increase the time of depressurisation. Consequently, the Figure 34 shows an asymptotic behaviour of the pressure, since the cabin pressure decrease when the time goes by. Moreover, it is visible that the discrepancies between the results of three different Mach numbers are bigger for a large opening.

7.2 Structural approach with the pressure load

The pressure field around and inside the cabin is strongly impacted by a depressurisation, but by the air speed of the airplane as well. Indeed, whereas the fast decrease of the cabin pressure leads to a strong flow close to the opening, the air-speed of the plane gives a rise to a low pressure zone on the exterior wall at the downstream flow as observed in the Charles's part (4.2). The simulation of inviscid compressible flows have shown the impact of the depressurisation on this low pressure pressure zone evolution:

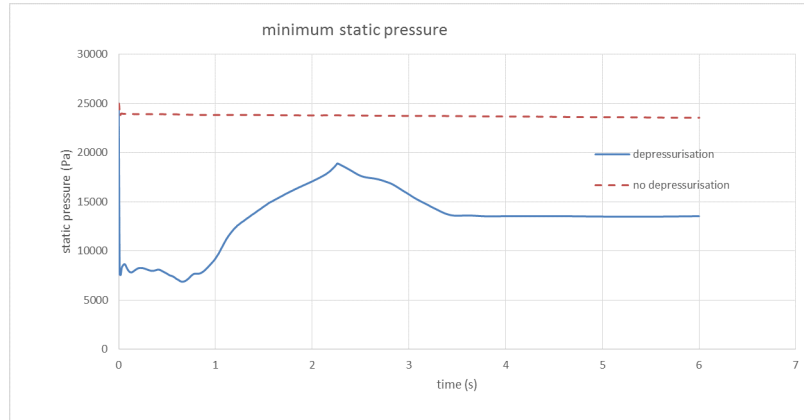


Figure 35: Minimum value of static pressure on Wall5-a

The results presented Figure35 shows the evolution of the minimum value of the pressure localised on the the external wall at the downstream flow i.e. the wall5-a for the mesh created on the ANSYS Meshing application. It is visible that an airflow around an open cavity will create a low pressure zone with a roughly steady value; With a depressurisation, this value is variable and always lower, at least for 6 second simulated. This same phenomena has been observed for other different speeds and opening sizes, as discussed further. For structural issues, the pressure load applied to the wall5 should be maximum before 1 second, when the pressure inside the cabin is still close to the initial high pressure, around 85000Pa, and the low pressure zone has appeared at the exterior surface. As the viscous stress components are here neglected, the only component studied is the normal stress caused by the pressures as visible on the inviscid momentum equation (1). With this assumption, the stress applied in a part of the wall will be related by the pressure difference between the inside and outside faces of this part, approached by (5).

$$\Delta p = p_{max_{Wall5-c}} - p_{min_{Wall5-a}} \quad (6)$$

It is more accurate to talk about pressure load applied on the wall, instead of stress that is affected by the structure of the cabin. Δp_{est} , being assumed as the first estimation of the maximum pressure load after a given period, $p_{max_{Wall5-c}}$ and $p_{min_{Wall5-a}}$ are calculated on Fluent with the function Vertex Maximum and Vertex Minimum, both for the pressure. The limitation of the relation (6) appears if the pressure gradient along the wall5 inside the cabin is considerable. Indeed, the assumption of a uniform pressure equal to $p_{max_{Wall5-c}}$ along the Wall5-b will tend to overestimate the maximum pressure at each time step, this difference will be discussed further. For all the cases simulated, minimum and maximum pressures evolution have been calculated in order to catch the time when the highest

pressure load occurs on the wall5. For an opening size at 1.27m and a Mach number of 0.82, the Figure 36 shows the evolution of the maximum pressure on the inside face of the wall5 (Wall5-a) and of minimum pressure on the external face of the same wall (Wall5-c).

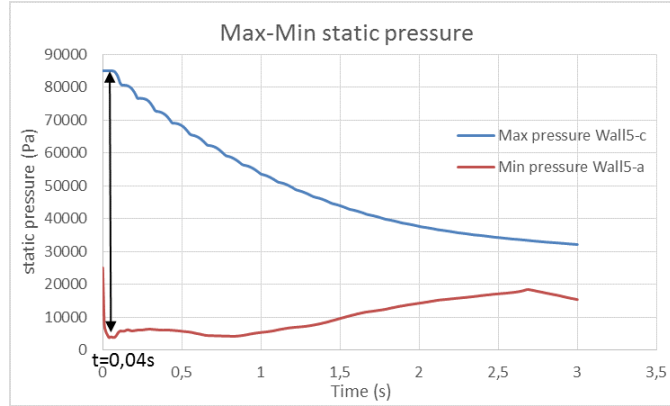


Figure 36: First estimation of the maximal pressure load

The maximum pressure has the same trend that the averaged pressure (Figure 34), unlike the minimum pressure evolution. The highest difference between those curves has been observed after a period T_{est} , such as $T_{est} = 0.04s$. The following figures 37 38 39 present the time evolution of Δp_{est} , firstly considerate as the maximum pressure load, for all the cases. The titles window, door, cargo door refer to the common openings visible on commercial airplanes.

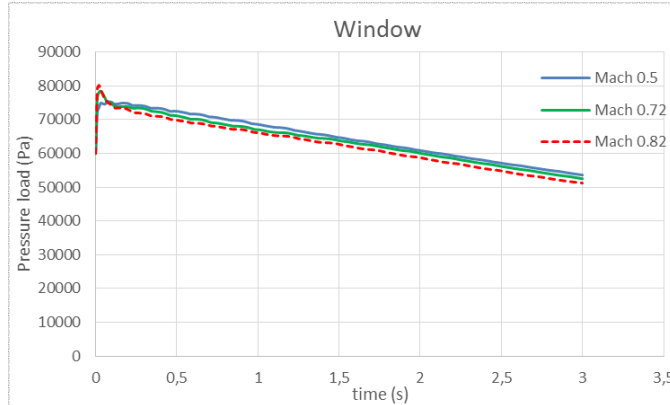


Figure 37: Estimated maximum pressure load with a window (0.3m)

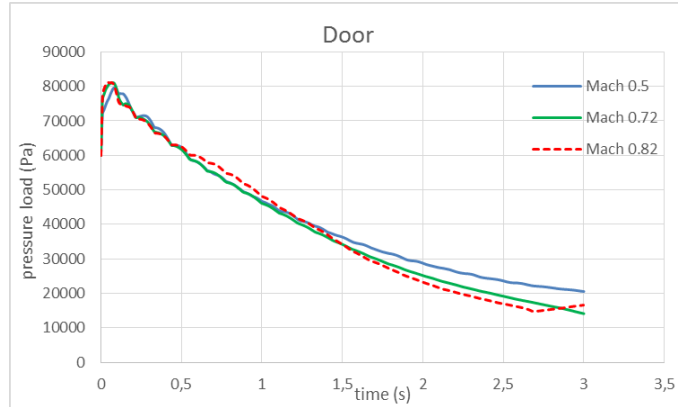


Figure 38: Estimated maximum pressure load with a door (1.27m)

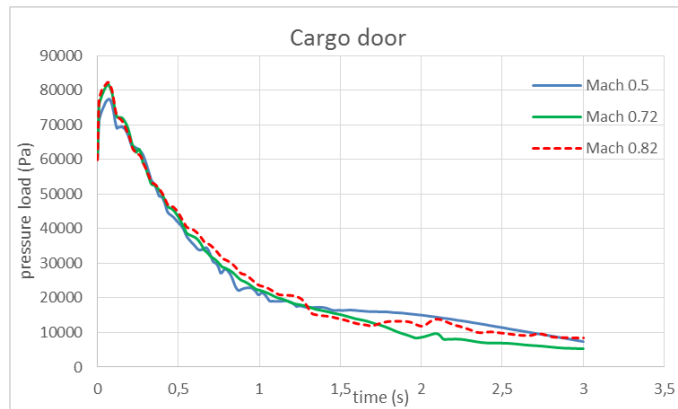


Figure 39: Estimated maximum pressure load with a cargo door (3m)

It has been observed that the maximum pressure load occurs at the very beginning, around $T = 0.1s$, and the value localised at this peak is roughly steady around 80000Pa. The discrepancies around this value are visible Figure 40. Moreover, a correlation is visible between the pressure load evolution and the pressure evolution inside the cabin (Figure 34) i.e. bigger is the opening faster the pressure load will reach a constant low value. This asymptotic value refers to a value of Δp_{est} calculated for a steady case with a flow around the cabin without any depressurisation.

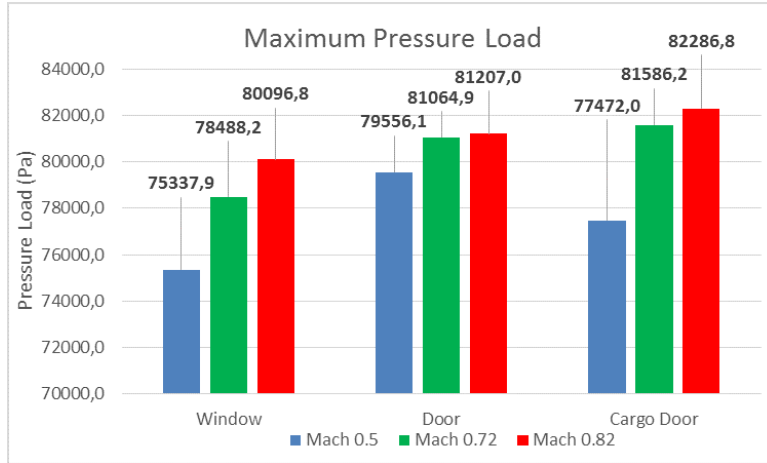


Figure 40: First estimation of maximum pressure load for all the cases

The Figure 40 shows that, despite a weak variation of the maximum pressure load, this value tends to increase with the Mach number, and with the opening size. Those results are linked to a specific time T_{est} when the maximum pressure load estimation has been calculated; However, the position of this load on the wall5 has to be identified. On the post processing ANSIS software CFD Post, two lines have been created, one for the inside face of the wall5 (Wall5-c) and the other on the external face (Wall5-a). For the specific time T_{est} , the pressure along those lines has been plotted in order to get the position where the maximum pressure load has been calculated. The time T_{est} is an estimation, and it has been observed that the real time T that refers to the maximal pressure load is close but different. For a size of 3m for the opening, and for a Mach number at 0.82, the Figure 41 present the pressure evolution along the lines referring to wall5-a and wall5-c, for three different times:

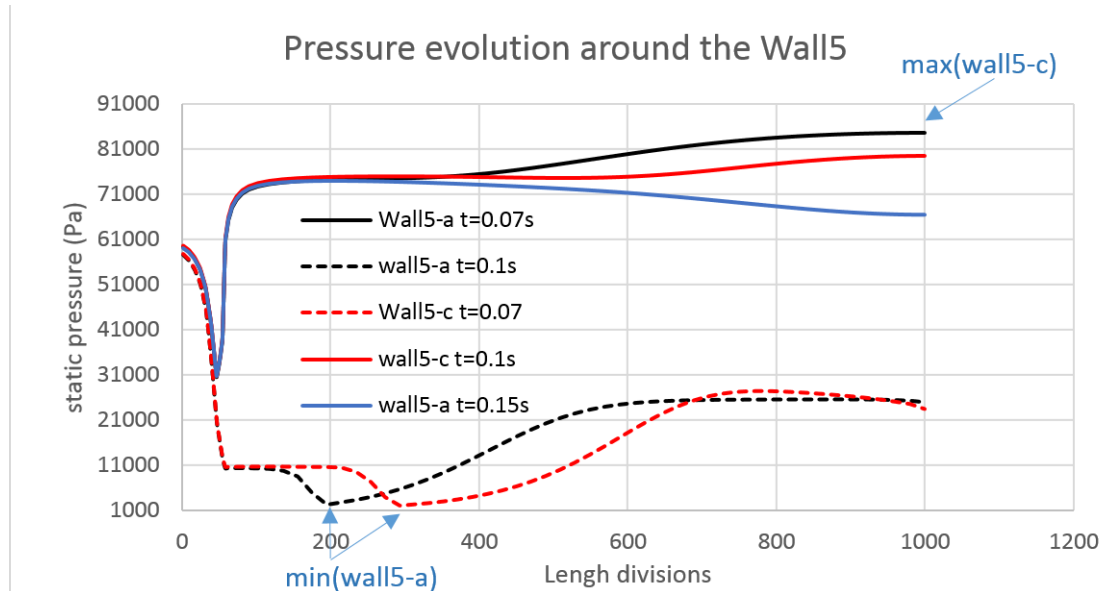


Figure 41: Limitations of the first estimation of the maximum load

The lines are sampled in a thousand of points. $t = T_{est} = 0.08s$ refers to the estimated

period of the maximum load. By plotting different time steps at the neighbour of T_{est} , a higher maximum load has been found for $t = 0.1s$. This difference is caused because of the cabin pressure gradient along the wall5-c. Indeed, despite that $\max(P_{wall5-c})$ keeps the biggest difference with $\min(P_{wall5-a})$ for $T_{est} = 0.08s$, the negative derivative (7), is not conserved along the wall5-a, especially at the location of $\min(P_{wall5-a})$ which hardly evolves from $T_{est} = 0.08s$ to $T = 0.1s$, that has been found as a more accurate time for the maximum load.

$$\frac{\partial \max(P_{wall5-c})}{\partial t} = \frac{\max(P_{wall5-c}^n) - \max(P_{wall5-c}^{n-\Delta t})}{\Delta t} \quad (7)$$

As the cabin pressure on the wall5 evolves faster far from the opening, the pressure gradient along this line evolves as well and after a while, the pressure far from the opening becomes smaller than close to the opening. This phenomena is visible on the previous Figure 41 at $t = 0.15s$. Using CFD post, the pressure evolution along the wall5-c and wall5-a has been calculated for several time steps neighboring the first estimation T_{est} , for all the simulation cases, in order to get a more accurate idea of when the maximum pressure load occurs on the wall5. The Figure 42 presents a comparison for the time, while the Figure 43 compares the maximum pressure load estimations:

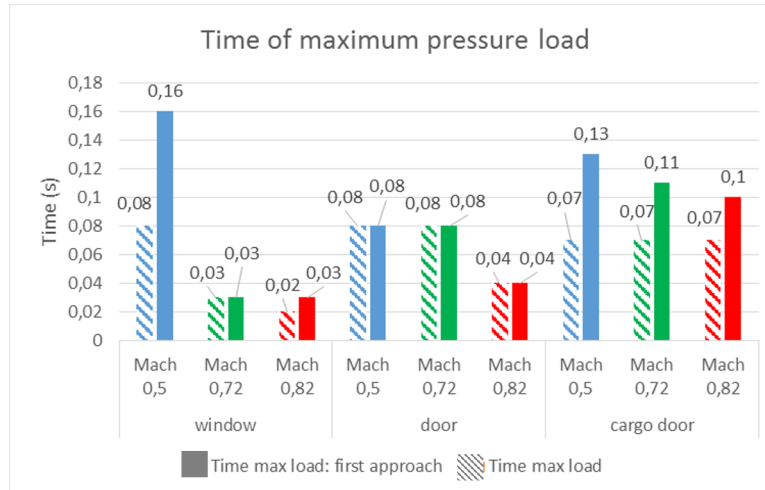


Figure 42: Impact of parameters on the time of the maximum load's apparition

For each case, the Figure 42 shows that the maximum pressure load occurs roughly at the same time around 0.1s. Regardless of the an exception at Mach 0.5 for a size of 0.3m, the time of the maximal loads tends to decrease with a higher Mach number, and increase with a larger opening. Regarding of the first approximation, using $\Delta p_{est}(6)$, the time has been underestimated for each case, with bigger differences with a large opening.

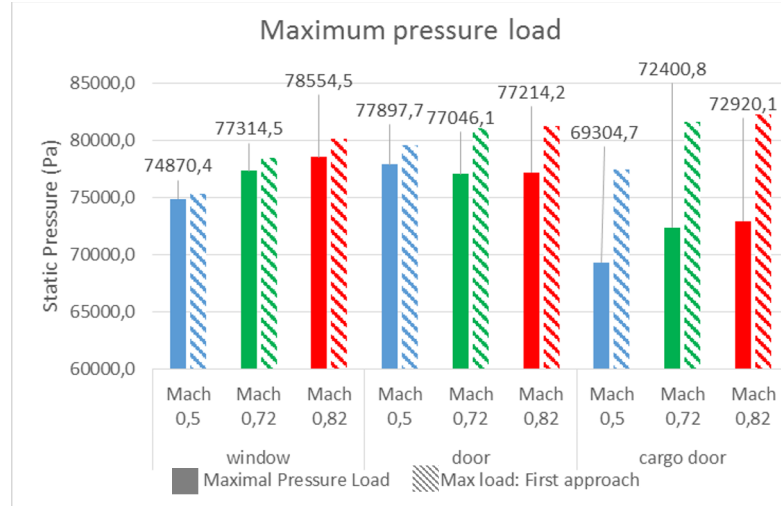


Figure 43: Impact of parameters on the time of the maximum load's value

The Figure 43 shows a maximum pressure load close to 80000Pa, so 20000Pa higher than in a normal cruising situation for an airplane at 35000ft. This maximum load tends to increase with a higher Mach number, and decrease with a larger opening. Regarding of the first approximation, using $\Delta p_{est}(2)$, all the maximal loads have been overestimated, with bigger differences for a large opening. Finally, from a better time and pressure estimation, the position on the wall5 of the maximum loads has been directly identified. The lines created on CFD post are sampled into a thousands of points, the Figure 44 presents a percentage of the position for each case. starting from 0% at the opening, to 100% at the corner of the cabin.

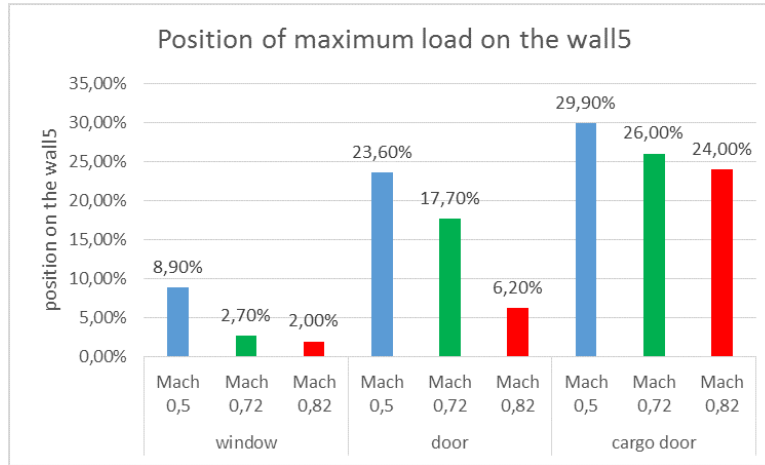


Figure 44: Impact of parameters on the time of the maximum load's position

The Figure 44 shows that higher is the Mach number, closer to the opening is the maximal load. Otherwise, this load increases with a larger opening. By taking into account the maximum pressure load with their corresponding time for different time steps, the Figure 45 shows, for a size of 3m, the impact of different Mach numbers on the maximal load's propagation, while 46 shows, for a fixed Mach number of 0.82, the impact of different size on this same propagation.

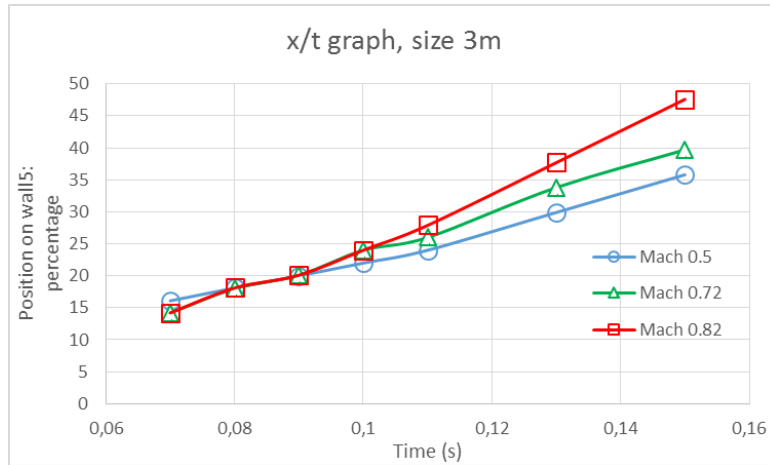


Figure 45: Impact of the Mach number on the maximum load propagation

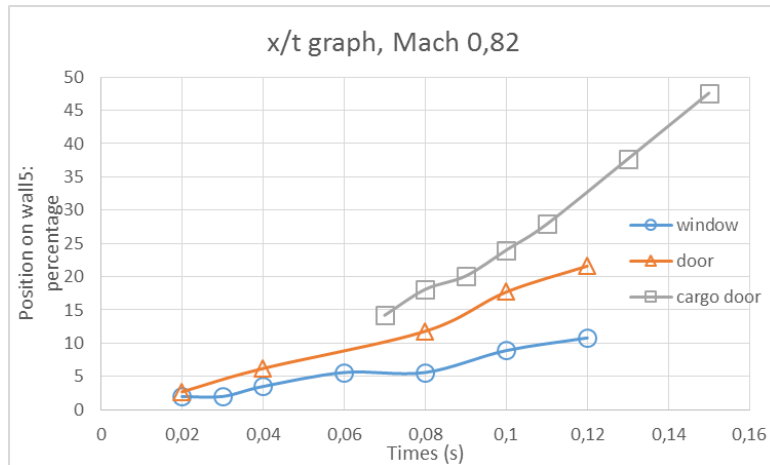


Figure 46: Impact of the opening size on the maximum load propagation

It is visible that the maximum pressure load propagates faster with a higher Mach number as well as that with a larger opening. If the structural issue, that gave a rise to the loss of an opening, is concerning a large section of the plane, the peak of pressure load that appears at the beginning of the depressurisation could trigger the loss of another opening.

8 Results Marin

In this section, we will study other physical models, and not only focusing on an inviscid model like the previous simulations. What leads us to try a different model was the expectations we had at the beginning concerning the profile of our results. We were expecting a peak of pressure on the walls at the very beginning of the simulation, before the drop of the pressure on the walls. As we have seen, with an inviscid model we don't observe at all this peak inside the cabin, where the average pressure is never above 85000 Pa (the initial pressure inside the cabin of the airplane). As a consequence, we decided

to change the physical model to see if we could have this peak at some point.

The first point was to introduce viscosity in our physical model, with a Sutherland law and turbulence by using URANS models : Spalart-Allmaras, k-E standart, k-E Realizable and finally k-w SST. We choose to work specifically with these URANS models for the following reasons : k-E Standart and Spalart-Allmaras are really well known models (even if Spalart-Allmaras is better for external flows), and k-w SST and k-E Realizable are recent models, and improvements from the previous ones, so those models are the most efficient RANS models. We kept the settings by default proposed by Fluent concerning the equations of these models. So including the inviscid one, five simulations were run in order to comment the differences caused by the choice of the physical model. Obviously, we used the same boundary conditions and initial conditions for each simulation (Mach number of 0.82, 25000 Pa and 220 K for the farfield, 85000 Pa and 293 K inside the cabin, operating pressure = 0 Pa), with an ideal-gas.

All these simulations are done with the first geometry we used, where we study a door for an Airbus A-350 (dimensions of the opening). We use the coarse mesh, with second order schemes for the flow, an explicit formulation as always, the ROE-FDS solver with the Least Square Cells Based method, and finally a second order implicit for the transient formulation. For the calculations, we used the settings defined previously ($dt = 0.001$, number of time steps = 3000, 80 iterations/time step). We plot with Matlab the comparison of the different results for each models on the interesting walls :

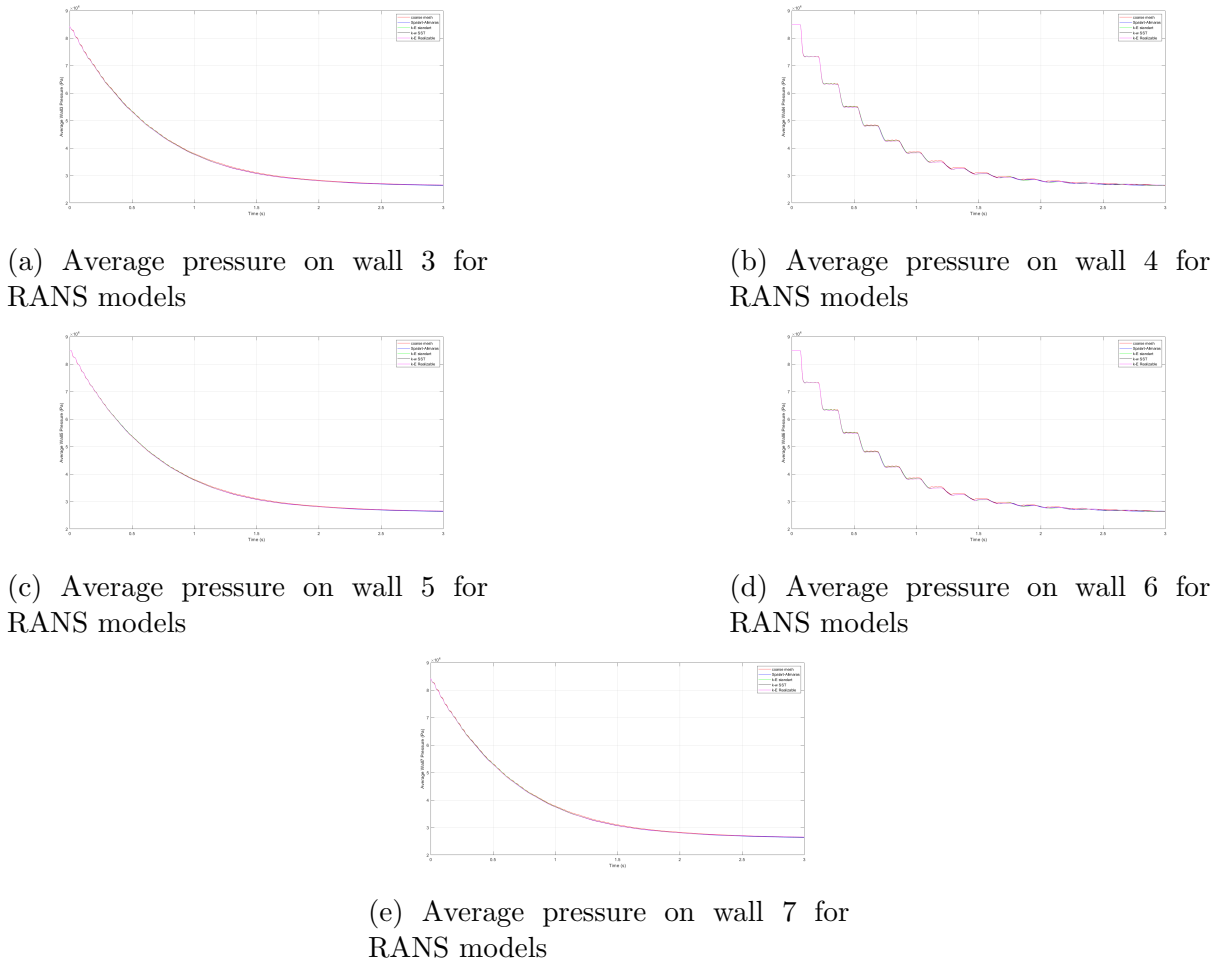


Figure 47: Study on RANS models

As we can see, using URANS turbulence models does not allow us to have a peak of pressure at the beginning of the simulation. We observe that all turbulence models (Spalart-Allmaras, k-E standart, k-E Realizable and k-w SST) give really close results, and also very close from the inviscid one. We get the same profiles, with a really small swift. Physically, these results seem good as we obtain something similar to the results with the inviscid model. However changing the physical model is not the solution to solve our problem and the difference is really small. Working with the inviscid model, as suggested as the beginning by our supervisor is the best idea at the moment and looking at the results with URANS models, there is no real need to introduce viscosity and turbulence. In the reality, the external flow has necessary turbulence so in a deeper study, it could be very interesting to run the simulations with URANS models, with an accurate study to choose exactly the right settings.

8.1 Study on the maximum pressure

Another idea to observe a peak of pressure on the wall is to plot the maximum pressure, rather than the average pressure. Indeed, the goal of the study is also to see if the material of the wall will resist to the peak of pressure we imagine (caused by the sudden

opening of the door/window), so working on the maximum pressure has a sense. Indeed, it is possibly this maximum pressure which will be problematic for the materials. With Fluent, there are two different ways to calculate the maximum pressure, so we tried both ([2]) : vertex maximum (The vertex maximum of a specified field variable on a surface is the maximum vertex value of the selected variable on the surface) and facet maximum (The facet maximum of a specified field variable on a surface is the maximum facet value of the selected variable on the surface). The main difference between facet and vertex is that facet are stored datas, while vertex are interpolated datas. We can plot both ways with Matlab and see what we are obtaining in terms of profiles and eventual peak of pressure :

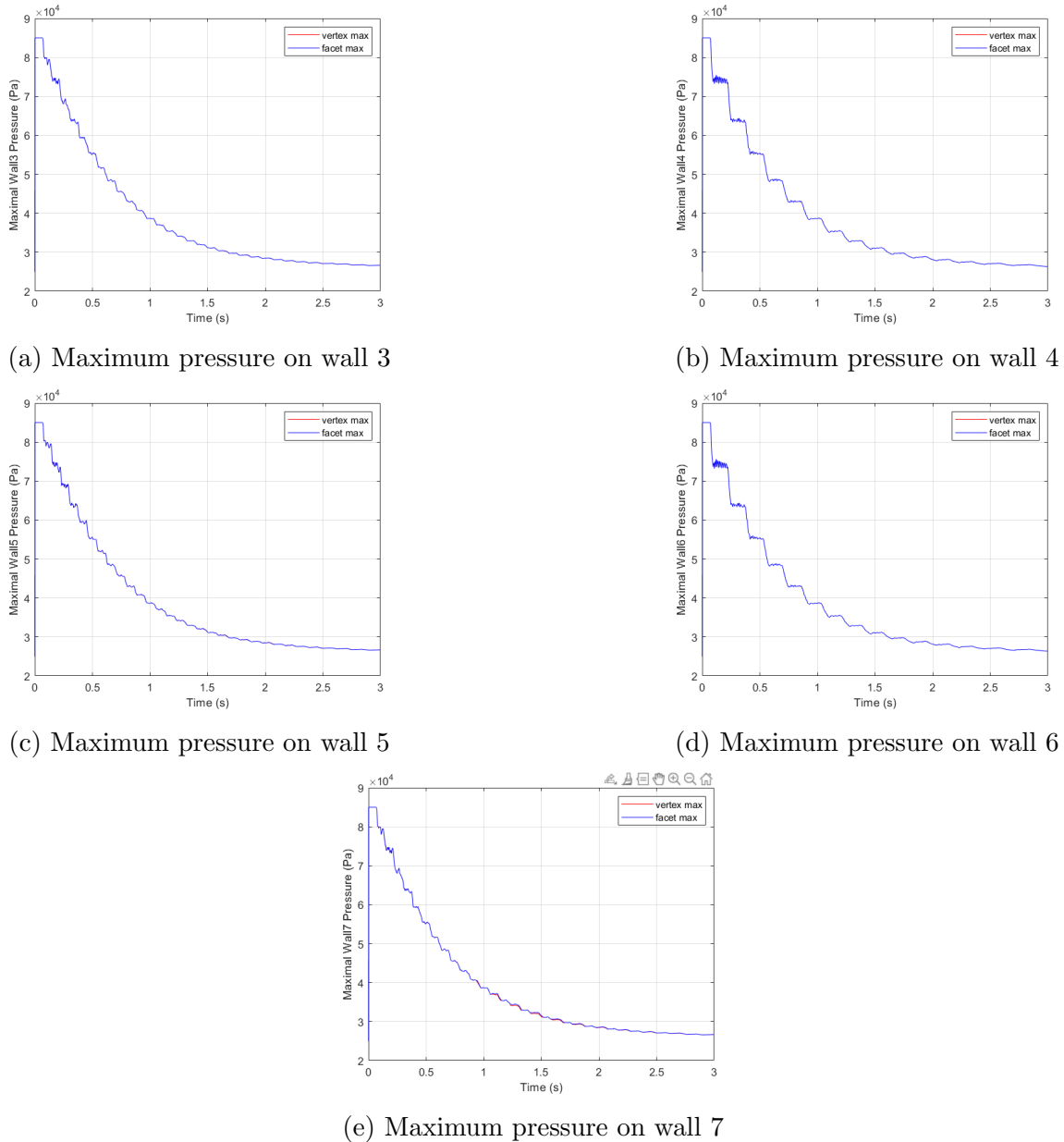


Figure 48: Study on the maximum pressure on the walls

The first observation we can make is that the two ways proposed by Fluent to calculate the maximum pressure on a wall give almost exactly the same results (except the first value which is calculated differently, 25000 Pa or 85000 Pa), so we don't have to pay attention to that anymore. The second thing to notice is that we fail again to obtain a peak of pressure at the beginning of the simulation. The maximum pressure never exceeds 85000 Pa (the initial pressure inside the cabin), and decreases quickly, exactly as the average pressure. Indeed, the values between the average pressure and the maximum pressure through the time are close, and we get the same profiles : the difference is that the maximum pressure is oscillating, while the plot for the average pressure is pretty smooth. It appears that if there is a peak to obtain, this is probably for a more specific geometry, or different conditions. But neither the physical model (inviscid or RANS models) nor the choice of the parameter we are working on (the average static pressure or the maximum static pressure) allow us to observe this peak.

8.2 3D mesh

In the last part of this group project, we tried to improve our geometry to have better results to work with, for example to observe this famous peak of pressure we are looking for, but also to be closer to the reality. Until now, all our simulations were done with a mesh in two dimensions. We tried to evolve this mesh to work in three dimensions. This is a very simple 3D model (realized with ICEM), but that can give us an idea of the results we can get by working in three dimensions. We kept exactly the same dimensions than for the previous 2D mesh (the one for the door of the A-350), but we added a height of 2 meters to go from the 2D to the 3D. To have an idea of the size of our mesh, this 3D mesh has 164198 cells, 506575 faces and 178480 nodes. Here you can see a view of this 3-D mesh, opened with Fluent :

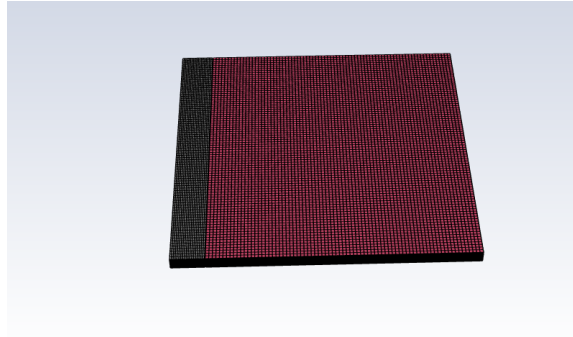


Figure 49: View of the 3D mesh

Inside the cabin, we are interested in the average pressure on seven walls inside the cabin when we work in three dimensions. We still have the walls 3, 4, 5, 6 and 7 which are the five walls we studied with the 2D model (as you can see in the scheme previously), and we have two additional walls corresponding to the ground and the ceiling. Using exactly the physical model and the Fluent settings we described previously, we run the simulations and plot the average pressure on these seven walls :

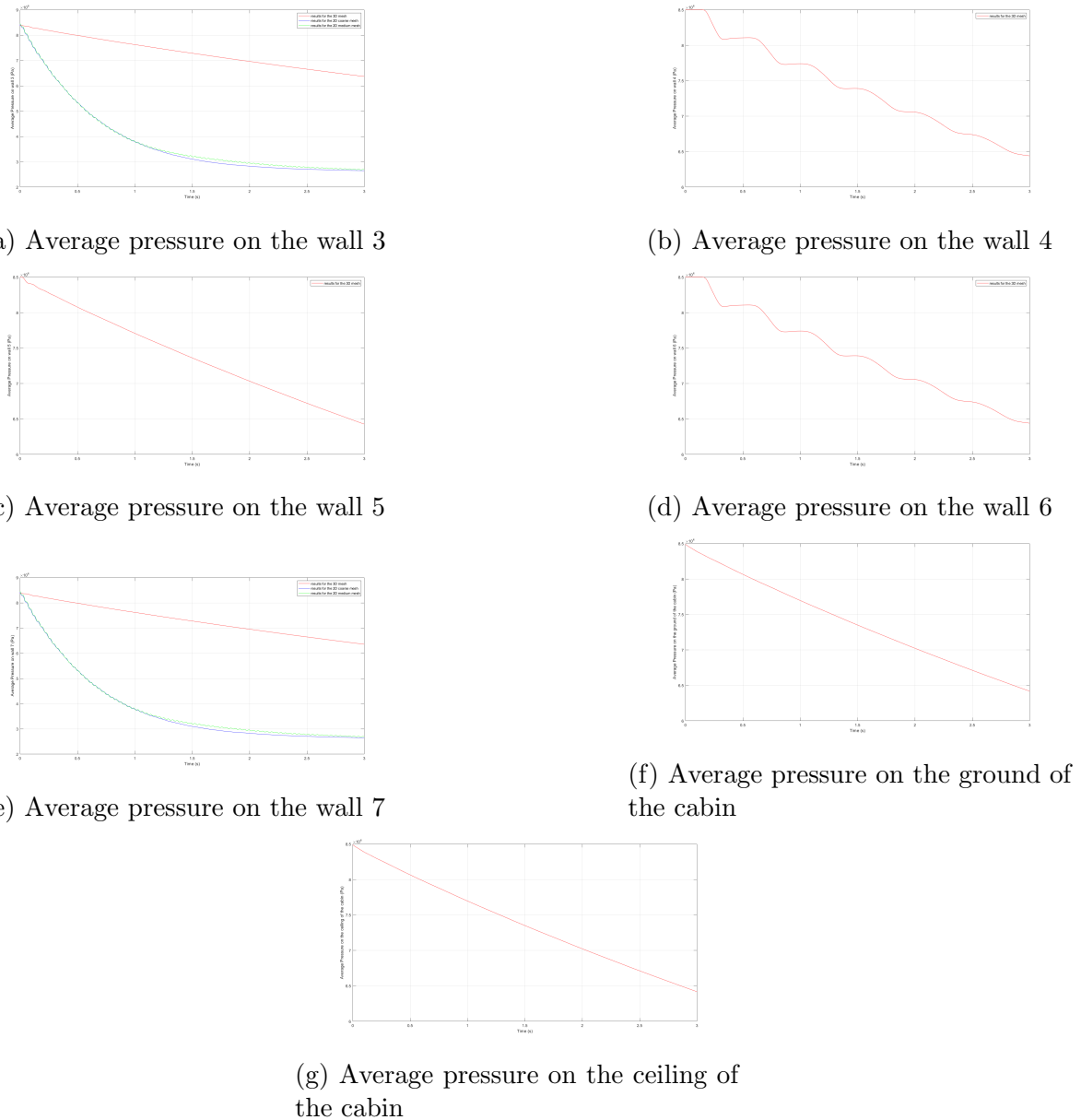
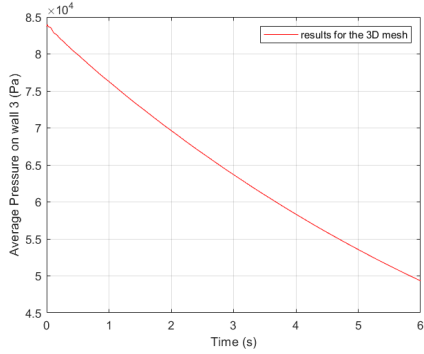
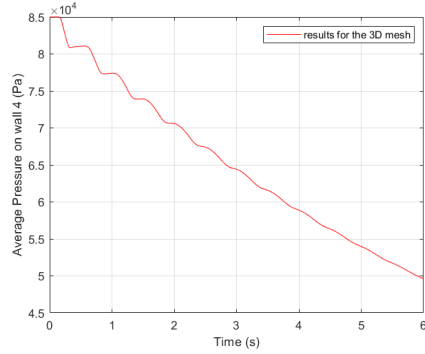
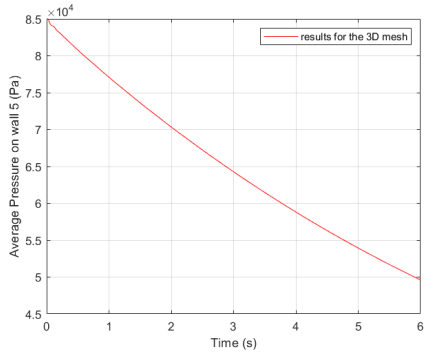
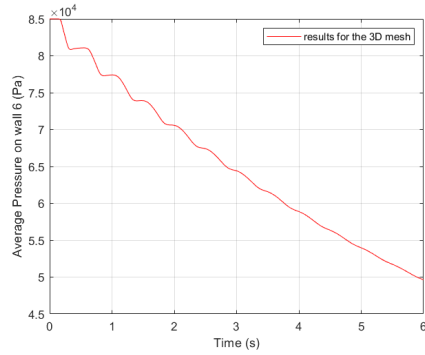
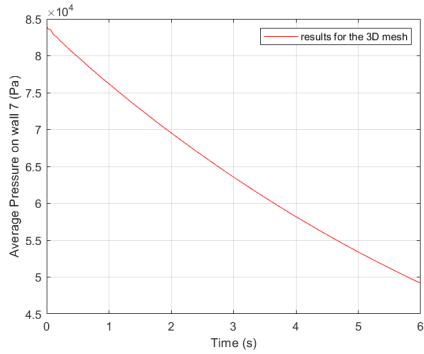
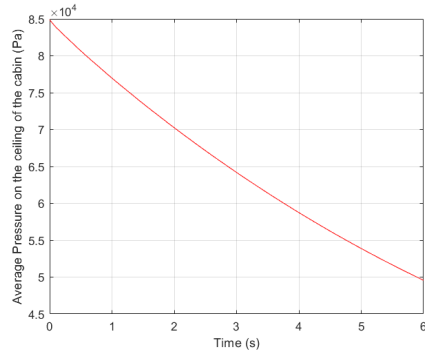


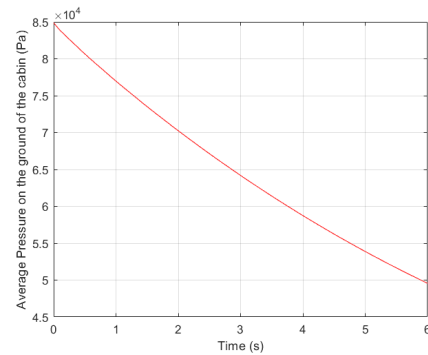
Figure 50: Study on the 3D mesh

Firstly we can observe the same profile for the average pressure between the 3D model and the 2D models : a decrease of the pressure through the time, without peak at the beginning. Basically, even if some of the average pressure are oscillating a bit (wall 4 and wall 6), we can observe than the evolution is the same on all the walls : we reach the same pressures at the same times. We observe also a symmetry between some walls : walls 6 and 7 give almost the same results, same for walls 6 and 4 (the sides), and something equivalent for the ceiling, the ground and the wall 5. If indeed we have this big depressurization with all the models (2D and 3D), there is still a big difference concerning the slope of the drop of the average pressure. With the 3D model, the drop is slower and less steep, so to reach the same pressure in the cabin, the 3D model will need a lot more time than the 2D models. To have an idea of the difference between the two models, we can compare for two walls (walls 3 and 7, the ones close to the door, which gives almost

exactly the same results) this average pressure. As we have seen with the GCI, the slope of the drop when we refine is a bit smaller (we can see it on the previous images), which means that the depressurization is slower. For the 3D mesh, this slope is even smaller than the slope of the finest mesh we work with. This slope is almost constant through the time. As an example, for the wall number 3, to reach 7000 Pa in our simulations, the 2D coarse mesh needs 0.20s, the 2D coarse mesh needs approximately the same time while the 3D mesh needs almost 2s, which is ten times more. So the 3D results are really different, and it is impossible to observe this peak of pressure we are looking for. It is impossible to know at that point of the study if these 3D results are better than the 2D results. It could be interesting to run a simulation for a bigger time to see if at one point, the average pressure decreases exponentially as the pressure for the 2D meshes. Just to check this information, let's try a simulation with a number of time steps of 6000 for a $dt = 0.001$, so we study the average pressure on the walls during 6s after the opening of the door (which is the double of the previous simulations) :

(a) Average pressure on the wall 3
(2nd simulation)(b) Average pressure on the wall 4
(2nd simulation)(c) Average pressure on the wall 5
(2nd simulation)(d) Average pressure on the wall 6
(2nd simulation)(e) Average pressure on the wall 7
(2nd simulation)

(f) Average pressure on the ground of the cabin (2nd simulation)



(g) Average pressure on the ceiling of the cabin (2nd simulation)

Figure 51: Study on the 3D mesh (2nd simulation)

We have seen that the speed of decompression is smaller for the model in three dimensions than what we observed in two dimensions. For the 3D model, this speed is almost constant during the first three second, while for the 2D models that was really different. When we simulate a bit more and run for a flow time of 6 seconds, we observe the same phenomenon that we had for the results with 2D models : the slope of the average pressure decreases gradually (in absolute value, the decompression is gradually slower). So the profile of the results we are looking for is apparently the same for all the models, in two and three dimensions : a strong decompression in the first seconds (which seems logic with the sudden opening of the door/window), and then a gradual stabilization of the pressure.

To end this part with the 3D model, it is really interesting to observe the contours of pressure around the opening with Fluent, for three different flow time (1s, 2s, 3s) :

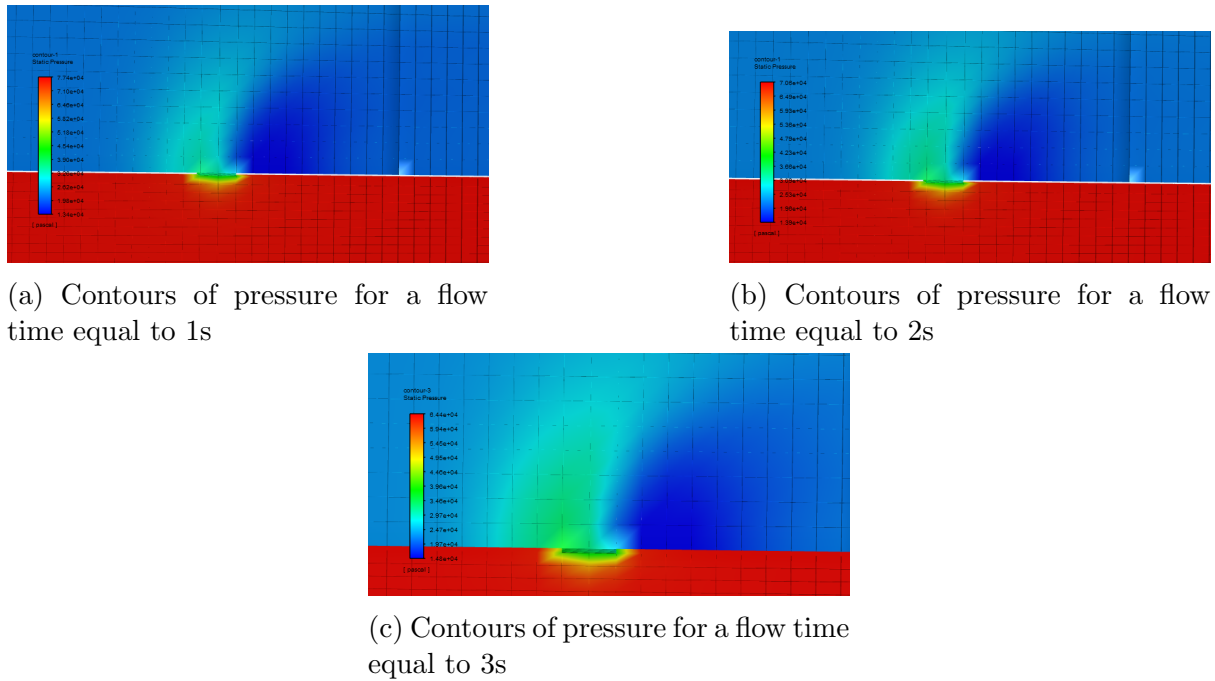


Figure 52: Contours of pressure with the 3D model

With the previous images we can observe several things (we know that the flow is coming from the left, going to the right). Outside the cabin near to the opening, the pressure against the wall is higher than the outside pressure (approximately 40000 Pa against 25000 Pa, so almost the double) at 3s after the opening of the door. So there is a brutal change of the pressure in these particular zone (over-pressure), which will logically leads to a potential issue for the structure. This higher pressure can be seen at the three different times (1s, 2s, 3s) and increases a bit through the time. Just after the door, we notice a zone where the pressure is really small near to the wall, still outside the cabin (13400 Pa against 25000 Pa for the outside pressure). We have a big depression in this zone. Once again the change of the pressure is huge and that will probably leads to a real issue. Besides, by observing the values, we see that at 2s then at 3s, the pressure in this specific zone increases a bit near to the wall (14800 Pa at 3s, 13400 Pa at 1s). So we can

imagine that there is this big depression created in this zone at the opening of the door, and that this depression is disappearing gradually through the time. We also notice, and this is a very essential point, that inside the cabin and close to the opening, we have big changes of pressure near to the wall. The structure close to the opening has to deal with violent changes of pressure through the time, and also very different pressures in a small distance at a fixed time. All of these changes are probably responsible for the issues on the walls inside the cabin. In conclusion, these contours show that the zone near to the door at the sudden opening is subject to violent changes of pressure, with different zones, and these violent changes are the potential issues for the the materials of the walls and the structure of the airplane.

In conclusion of this part, the model in three dimensions gives maybe better results, but we still have the same profiles, so the 2D models were already pretty good and not off topic. However working with a 3D model is obviously more accurate, closer to the reality (more accurate geometry). We observe differences concerning the speed of the drop of pressure, smaller for the 3D model, and if it is difficult to explain these differences, the trend we observe when we refine in 2D let us think that the 3D results are better than the 2D results we got (having a smaller slope seems to be closer to the reality). Having access to a real case is really difficult, as the opening of the door during a flight is very dangerous, but setting up an experiment for this certification problem could be nice, as we are still not sure we have the right profiles for this average pressure (for example not having the peak of pressure at the beginning). To simulate with Fluent more exactly this case, it will be essential to create a more realistic geometry (right now we have the right dimensions for the opening, but we probably need to build exactly the right dimensions for the cabin to observe the average pressure correctly). Having access to the good dimensions is not an easy task, but that will be probably the key to create a good 3D model and run an accurate simulation. The geometry of the cabin has certainly an essential role in this study.

9 Future work

As this project lasted only one month and half, with big external issues like the coronavirus crisis, and has only few explanations of the phenomenon in the literature, there is still a lot of things to improve to have access to better results concerning our study.

The first thing to improve in the future is creating a more accurate mesh, in three dimension. We realized that the geometry of the cabin has probably an impact on the results we observe, and not only the geometry of the opening. So it could be essential to create exactly the geometry of a cabin (for an Airbus A-350 for example), to see if the results change or stay very close the ones we got with the simple 3D model. In order to do that it is necessary to have access to the real dimensions of the airplane, which is not always easy.

Secondly, as we are working on a certification problem, it could be really interesting to make an accurate structural study. The goal will be to choose some specific points in the geometry, calculate the difference of pressure and see if the materials of the walls are able to deal with these differences of pressure. The choice of these specific points has to be defined (probably all around the opening) and it is necessary to have access to the specific properties of the materials and his resistance to the pressure. In Giorgio's part, we already give an idea of the location of some specific points to work with, and in Sevan's part we began to talk about the load on the walls of the opening. The goal of this study will be to verify if there is a real problem for the walls, or if in case of problem these walls will be resistant enough to these difference of pressure.

Linked to the previous idea, a study on the aerodynamic forces experienced by the walls inside the cabin could be great. Once more, the goal is to see if the walls are able to deal with these forces without problem.

10 Conclusion

To conclude, our study has demonstrated and highlighted several results on different phenomena such as pressure measurement methods and simulations' criteria. Structural analysis and 3D extend the study.

Local and Global measurements do not give the same information. Local measurements highlight pressure peaks at the opening and pressure differentials close to walls but suffer from oscillations which can be reduced via refinement. Pressure tendencies obtained via wall measurements are smoother and show accurately the global pressure trend inside the cabin. Refinement impacts pressure result in term of oscillatory behavior, pressure decrease rate and peaks' value at the opening. A brief study of the opening's length has demonstrated impact on decompression rate. The larger the opening is, the quicker is the decompression.

With our model, mesh Convergence study showed that the convergence of the results are easy to obtain in the first time steps straight after the loss of the door. However, pressure results are still improving for the later time steps if a mesh refinement is performed. As this study focuses on the first time steps, it makes sense to use a relatively medium mesh which is enough to give a good precision for the first time steps and a satisfying precision for all of the other time steps with a very reasonable computational time. The cabin decompression is smooth on all of the cabin walls as pressure drops towards balance. Small peaks of pressure have been shown on the door frame. On the exterior fuselage, an area of over pressure forms upstream the door, and an area of under pressure forms downstream the door. These elements show that a decompression could be dangerous for the structure of the aircraft fuselage. Secondly, simulations showed that the lower the plane flies, the slower the decompression is. Therefore the decompression behavior mainly depends on the difference of pressure between the cabin and the exterior air. Additionally, this parametric study illustrates that the length of the opening (cargo compartments, doors, windows) influence the time of decompression of the cabin. Obviously, the larger the opening is, the quicker the decompression will be. There is no peaks of pressure at the very beginning of the cabin, neither during the entire time of decompression. However, oscillations during this decompression are noticeable. Those oscillations could be the real danger for the structural integrity of the airliner, further studies on this behavior could be interesting to perform. Furthermore, the results shows that the position of the opening zone has a direct effects on the cabin pressure behavior. This effects are clearly noticed in the front and back walls respectively. Similar results are obtained between two dimensions and three dimensions, with a decompression without any peak of pressure. Without some results (or experiments) to compare and validate, it is impossible to say at that point if the 3D results are better than the 2D results or not. We notice that the decompression is really faster with the 2D model than the 3D model. In 3D, we observe an over-pressure and a decompression around the opening. Indeed, there are violent changes of pressure in space (small distance around the cabin) and in time (during the first seconds of flow time) that can have an impact on the structure of the airplane and the materials of the walls. The next step will be to create a more accurate 3D geometry of the cabin.

Several tests have been made for three Mach numbers and three sizes for a centered opening. For averaged pressure evolution on each wall inside the cabin, differences given

by different Mach numbers are bigger by increasing the size of the opening. Inside the cabin, the pressure gradient along the wall5 evolves when the time goes by, so the maximum static pressure is not localised far from the opening after a while. For future structural approaches, the maximum pressure load occurs on the wall5 i.e. the wall localised at the downstream flow where the local low pressure appears. The maximum load has been found at the beginning of the depressurisation, between 0.02s to 0.16s for each cases and the value is estimated between 69305Pa to 78555Pa, that means almost 20000Pa more than in cruising condition. This maximal load appears at a certain distance from the opening that depends of the Mach number and the size of the opening. Referring to the results found, higher is the Mach number, closer from the opening is the maximum load; Bigger is the size, further this maximum loads occurs from the opening. Otherwise, the load keeps a quite high intensity and propagates at a speed that depends of the parameters, this propagation speed increases with the Mach number and the size of the opening.

11 References

References

- [1] *A350 aircraft characteristics airport and maintenance planning*. Airbus. Rev 2019. URL: <https://www.airbus.com/aircraft/support-services/airport-operations-and-technical-data/aircraft-characteristics.html>.
- [2] *Ansys, 20.3.1 Computing Surface Integrals*. ANSYS. 2009. URL: <https://www.ansys.com/project/neptunius/docs/fluent/html/th/node416.htm>.
- [3] Nihad E Daidzic and Mathew P Simoned. “Aircraft Decompression with Installed Cockpit Security Door”. In: (2010).
- [4] Alfonso Pagani and Erasmo Carrera. “Geodynamics of rapid and explosive decompressions of pressurized aircraft including active venting”. In: (2015).
- [5] John W.Slater. *NPARC Alliance CFD Verification and Validation Web Site*. NASA. 2008. URL: <https://www.grc.nasa.gov/WWW/wind/valid/tutorial/spatconv.html>.